A New Fast Method for Calculating Non-linear Wave Loading on Offshore Structures

Dr. Jun Zang, University of Bath, UK

Outline

- Background
- What we learnt from non-linear wave interactions with monopile structures?
  - Importance of high order wave loading components
  - New fast approach to calculate non-linear wave loading
- Comparisons of the performance of numerical methods

Wave interaction with gravity base structure with a caisson

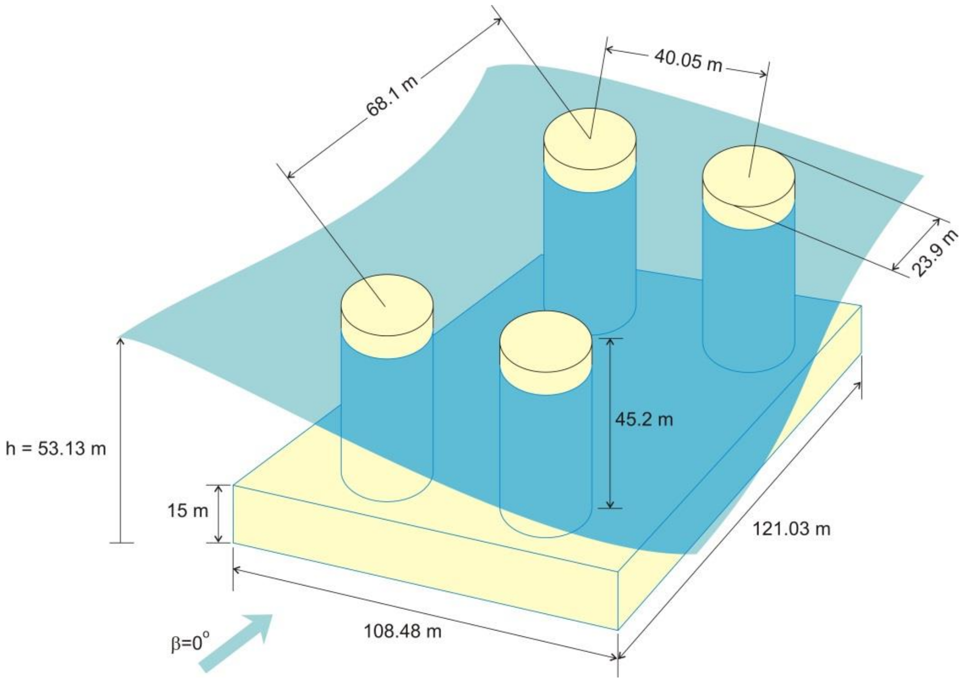

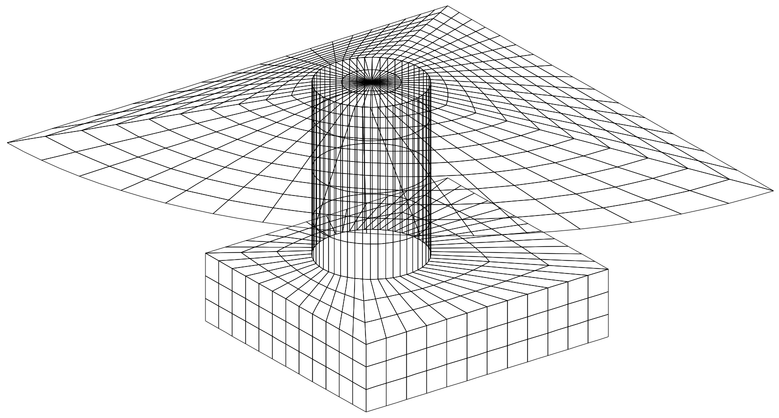

WALKER, D.A.G., EATOCK TAYLOR, R., TAYLOR, P.H. and ZANG, J. (2008)

Wave diffraction and near-trapping by a multi-column gravity base structure. *Ocean Engineering*. 35(2) pp 201-229.

Free surface elevation between the *rear legs*

(for 11m incident focused wave group)

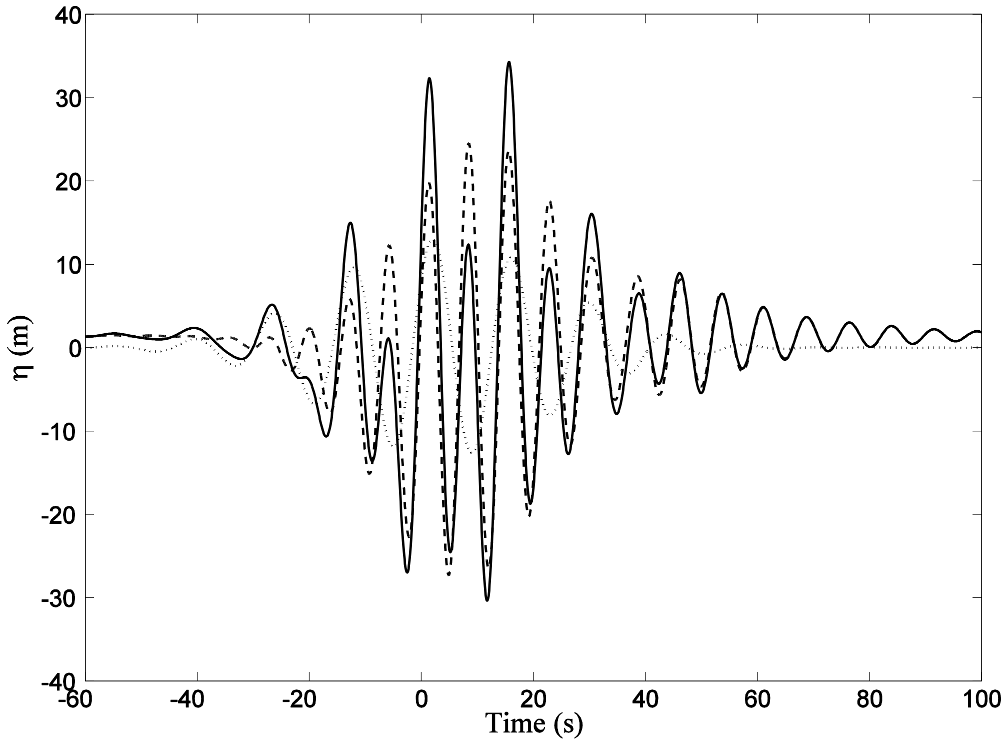

••••• $h^{(1)}$;

------ $h^{(2+)}$;

—— $h^{(1+2)}$

Wave interaction with a FPSO

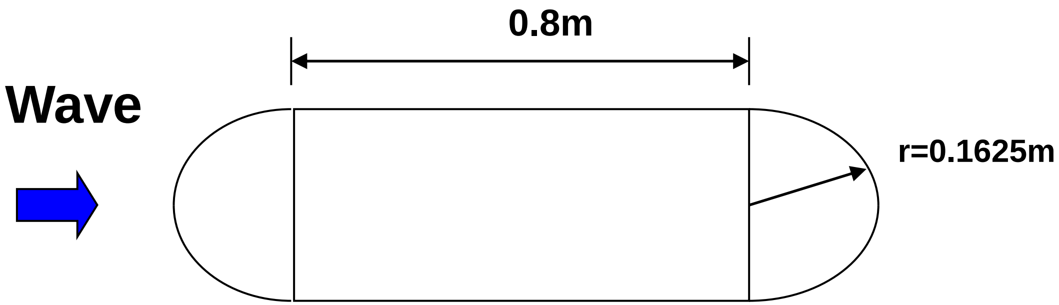

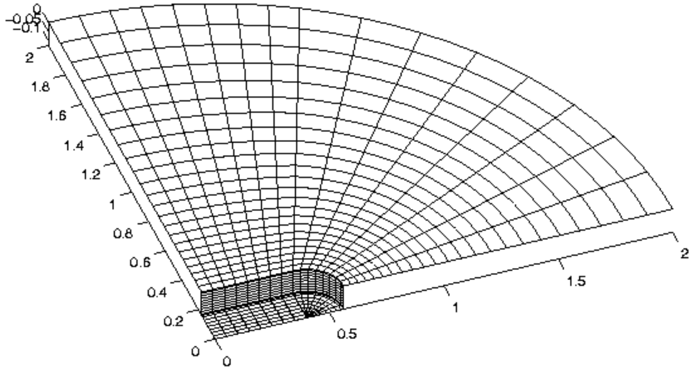

Zang J, Gibson R, Taylor PH, Eatock Taylor R, Swan C. (2006).

Second order wave diffraction around a fixed ship-shaped body in unidirectional steep waves. *Journal of Offshore Mechanics and Arctic Engineering*. 128 (2). pp. 89-99.

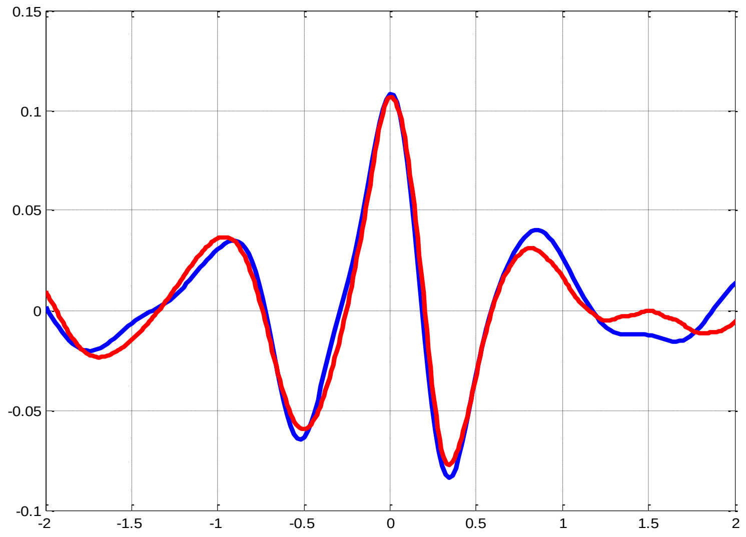

numerical non-linear free surface
experimental non-linear free surface

numerical incoming wave
numerical 1st-order free surface
numerical non-linear free surface

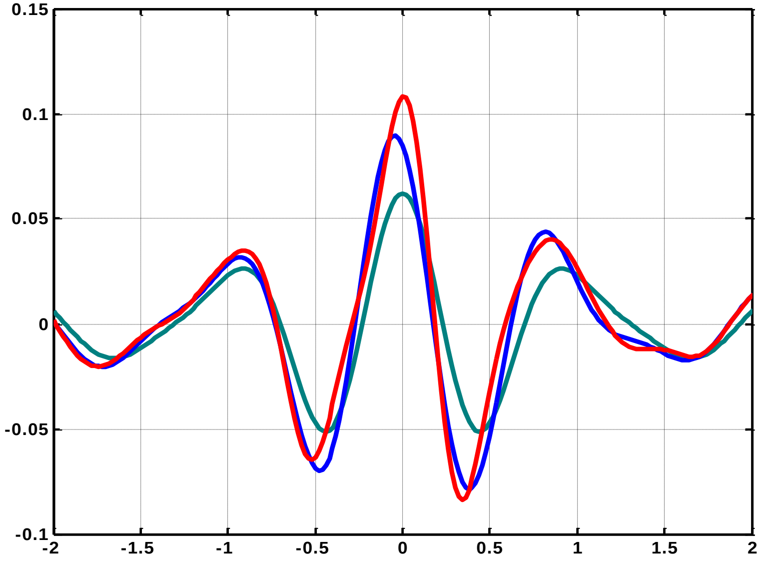

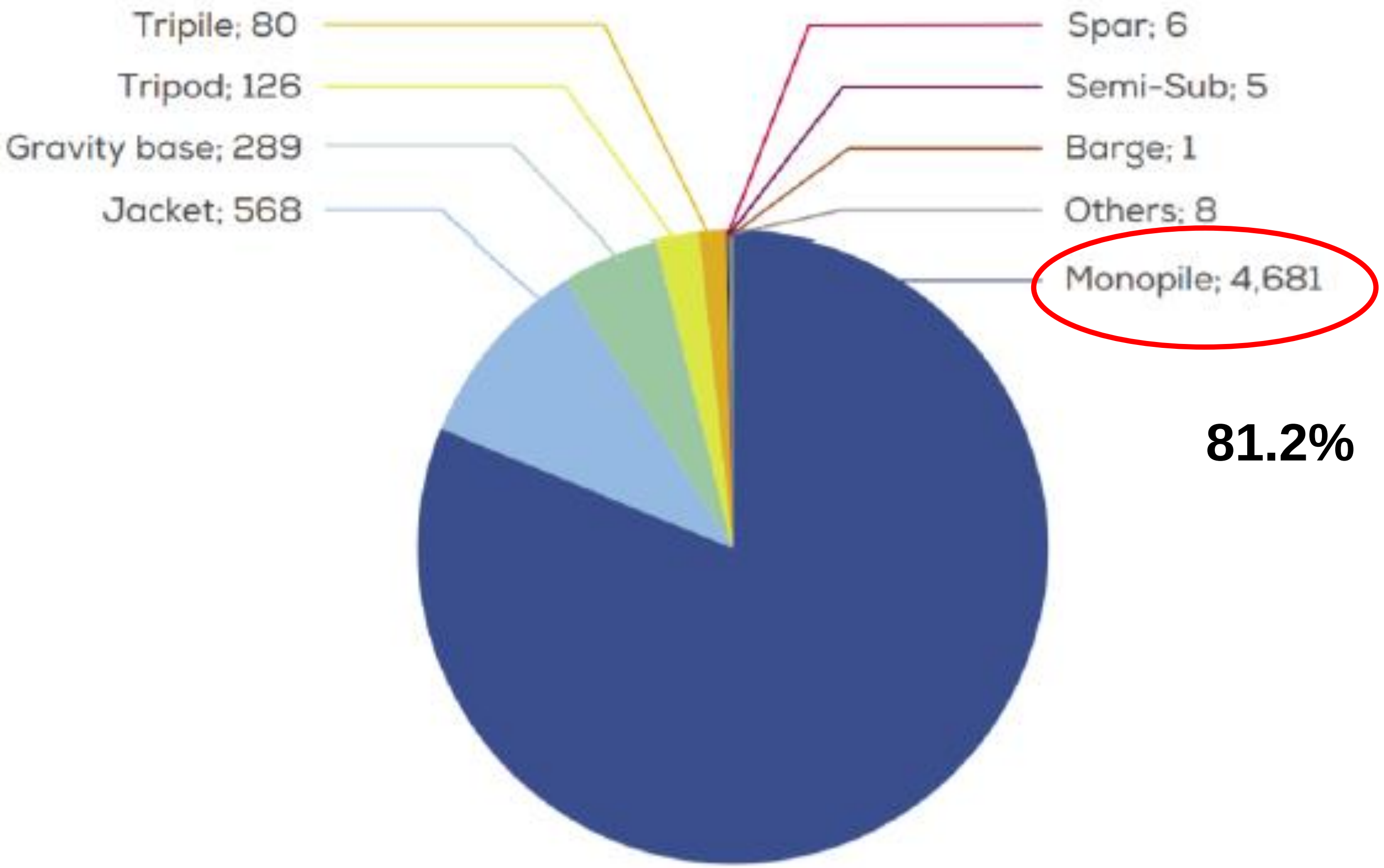

Cumulative number of OWT foundations insta structure type (Wind Europe 2021)

Violent wave impact on offshore wind turbine foundations

(Credit: Siemens Gamesa)

Violent wave impact on offshore wind turbine foundations

Water depth d = 0.5m

Cylinder radius R = 0.125m

We want to investigate

- how important the high order wave loadings are
- how the non-linear loading is distributed.

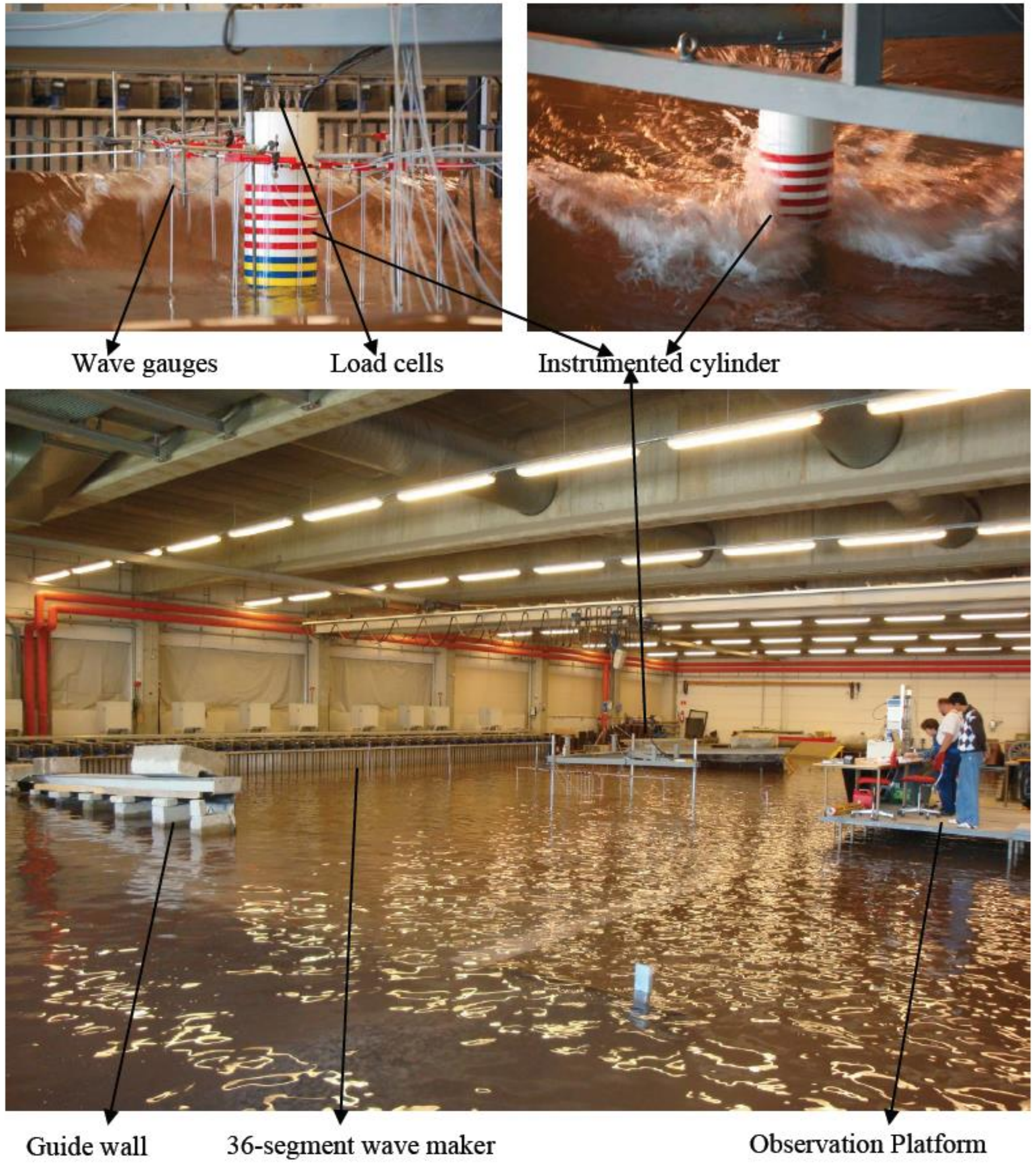

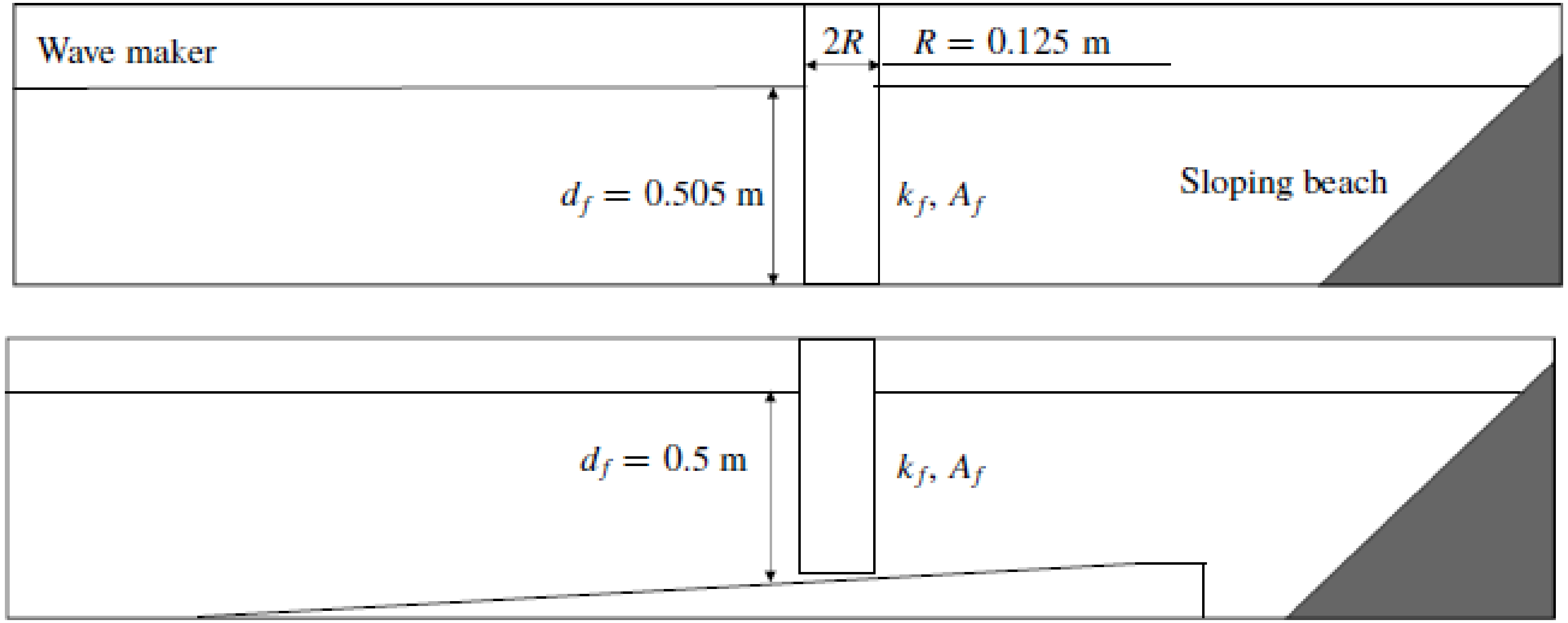

Chen, L.F., **Zang, J.,** Taylor, P.H., Sun, L., Morgan, G.C.J., Grice, J., Orszaghova, J. and Tello Ruiz, M.

An experimental decomposition of nonlinear forces on surface-piercing column: Stokes-type expansions of the force harmonics

Journal of Fluid Mechanics, 2018

The incoming wave conditions

f_p (Hz)	k_f (m^{-1})	$k_f R$	$k_f d_f$	Flat bed cases		Sloping bed cases	
				A_f (m)	$A_f k_f$	A_f (m)	$A_f k_f$
0.49	1.505	0.188	0.760	0.013	0.020	0.018	0.027
				0.028	0.042	0.036	0.054
				0.056	0.084	0.070	0.106
				0.081	0.122	0.096	0.144
				0.101	0.152	0.111	0.167
						0.119	0.179
0.61	1.971	0.246	0.995	0.026	0.051	0.032	0.063
				0.052	0.103	0.061	0.120
				0.090	0.177	0.105	0.207
0.82	2.985	0.373	1.507	0.023	0.070	0.027	0.081
				0.041	0.122	0.049	0.146
				0.075	0.224	0.079	0.237
				0.090	0.269	0.099	0.296
1.22	6.020	0.753	3.040	0.013	0.080	0.015	0.091
				0.023	0.139	0.025	0.150
				0.041	0.246	0.044	0.265
				0.049	0.293	0.050	0.297

Importance of high frequency wave loading

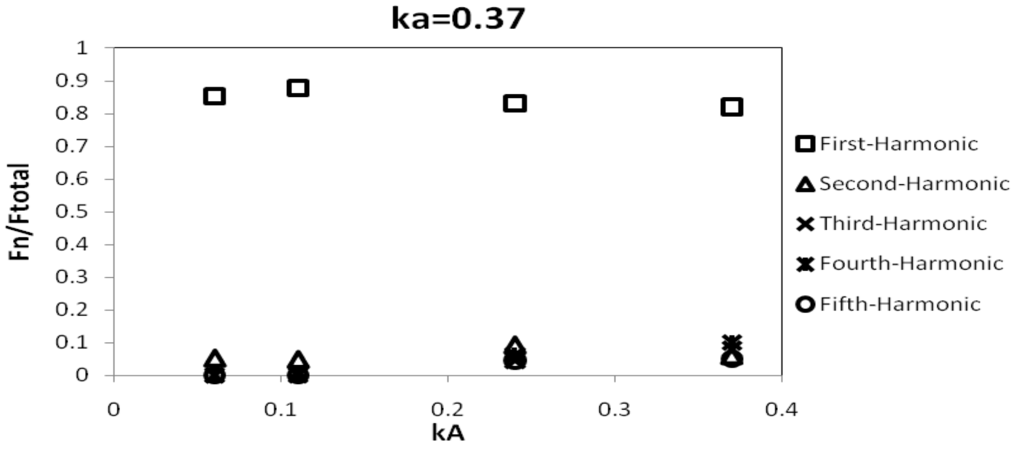

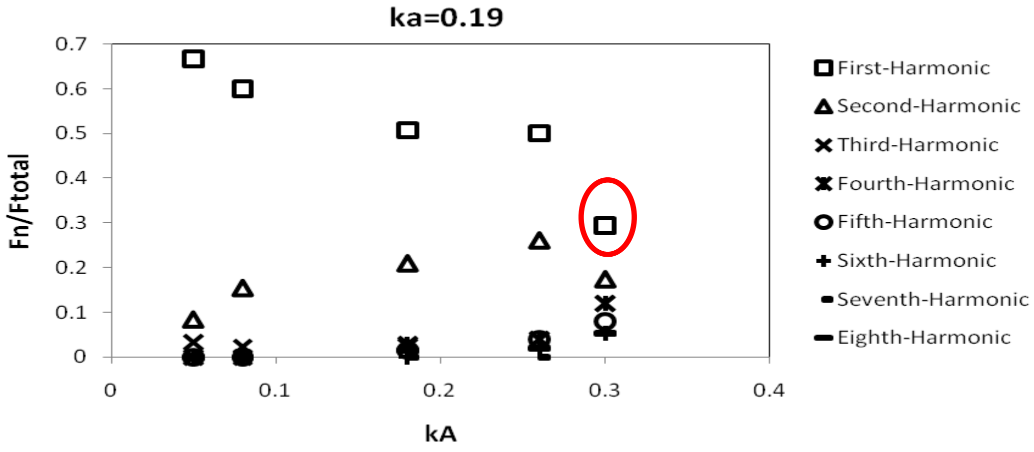

Water depth d=0.5m

Cylinder radius a=0.125m

k: wave number

a: cylinder radius

A: wave crest

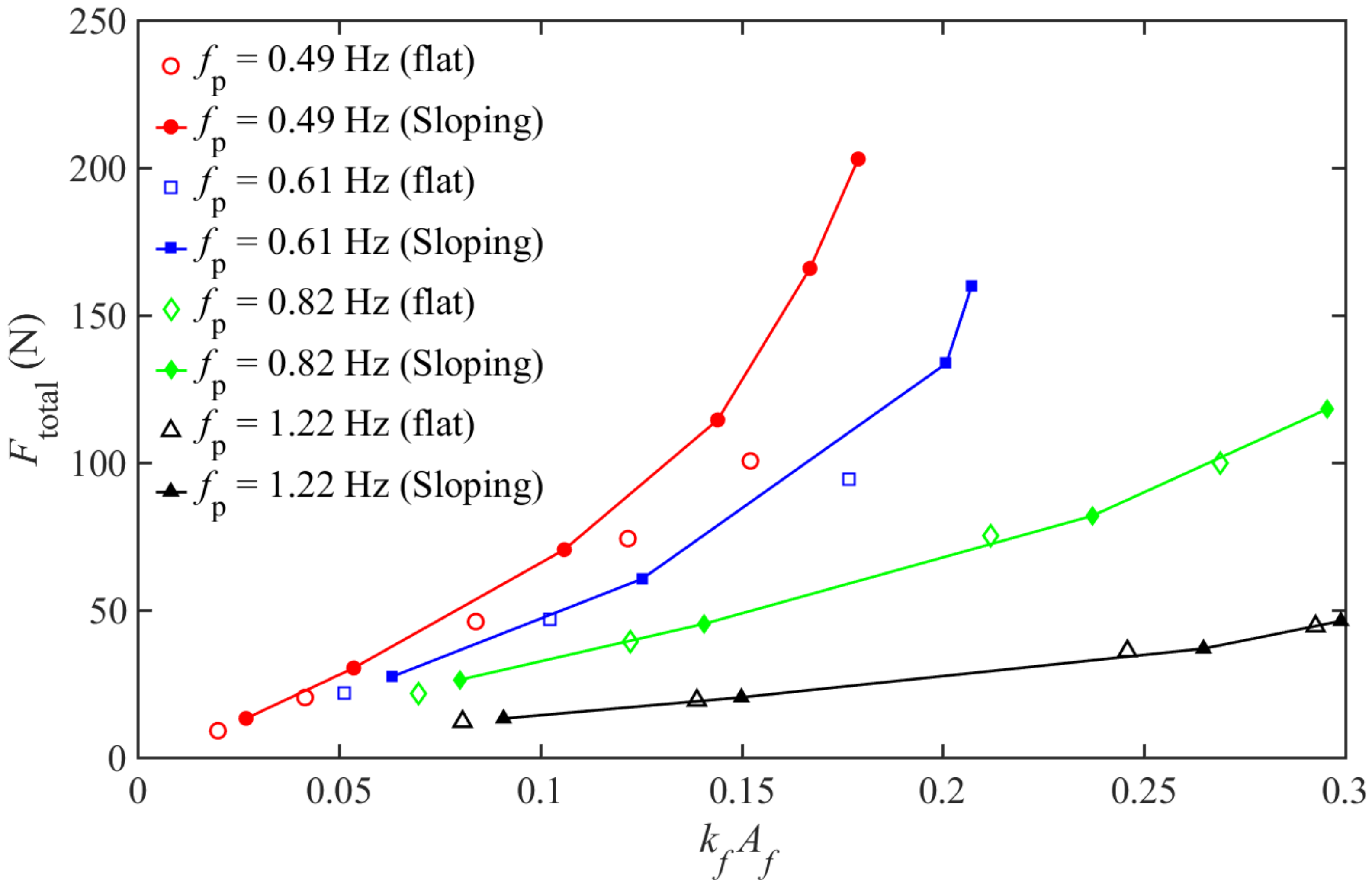

f_p = 0.49 Hz (flat)
f_p = 0.49 Hz (Sloping)
f_p = 0.61 Hz (flat)
f_p = 0.61 Hz (Sloping)
f_p = 0.82 Hz (flat)
f_p = 0.82 Hz (Sloping)
f_p = 1.22 Hz (flat)
f_p = 1.22 Hz (Sloping)
F_{total} (N)
$k_f A_f$
0
50
100
150
200
250
0.05
0.1
0.15
0.2
0.25
0.3

Note: Size of 2nd, 3rd and 4th force harmonics

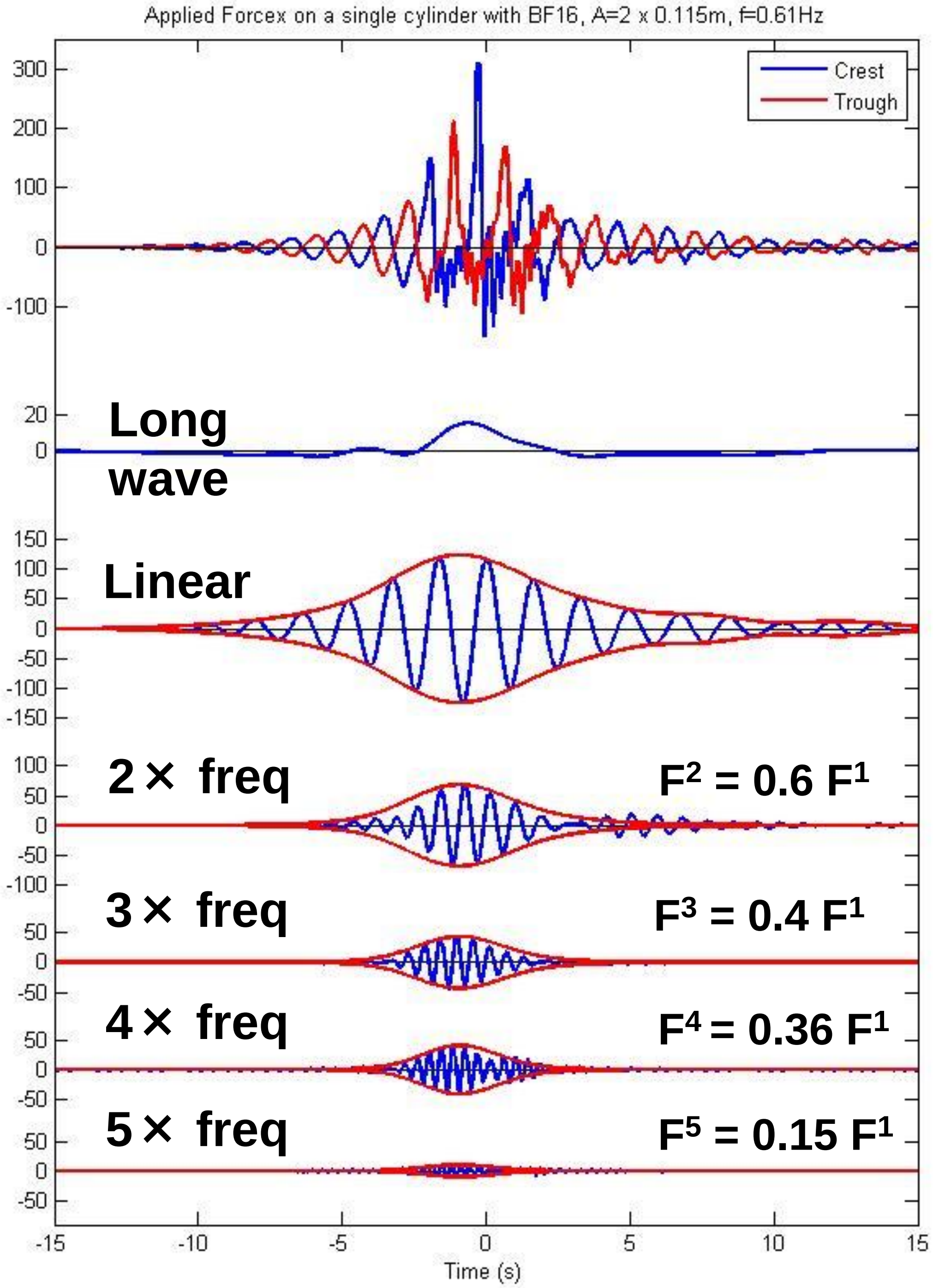

For a regular wave, the surface elevation can be written in non-dimensional form as

$$\frac{\eta}{A} = \cos\theta + S_{EE2}\left(\frac{A}{R}\right)\cos(2\theta) + S_{EE3}\left(\frac{A}{R}\right)^2\cos(3\theta) + \cdots ,$$

Where the linear phase function is $\cos(\theta)$

the wave amplitude is A

the radius of the cylinder is R

the second-order coefficient is S_{EE2}

the third-order coefficient is S_{EE3}

For a wave group, the free surface elevation is approximately as

$$\frac{\eta}{A} = \eta_1 + S_{EE2}\left(\frac{A}{R}\right)[\eta_1^2 - \eta_{1H}^2] + S_{EE3}\left(\frac{A}{R}\right)^2[\eta_1(\eta_1^2 - 3\eta_{1H}^2)] + \cdots .$$

By generating both crest and trough focused wave groups, odd and even harmonics can be calculated by

$$\frac{1}{2}\left(\left(\frac{\eta}{A}\right)_{crest} - \left(\frac{\eta}{A}\right)_{trough}\right) = \eta_1 + S_{EE3}\left(\frac{A}{R}\right)^2[\eta_1(\eta_1^2 - 3\eta_{1H}^2)] + \cdots$$

$$\frac{1}{2}\left(\left(\frac{\eta}{A}\right)_{crest} + \left(\frac{\eta}{A}\right)_{trough}\right) = S_{EE2}\left(\frac{A}{R}\right)[\eta_1^2 - \eta_{1H}^2] + \cdots .$$

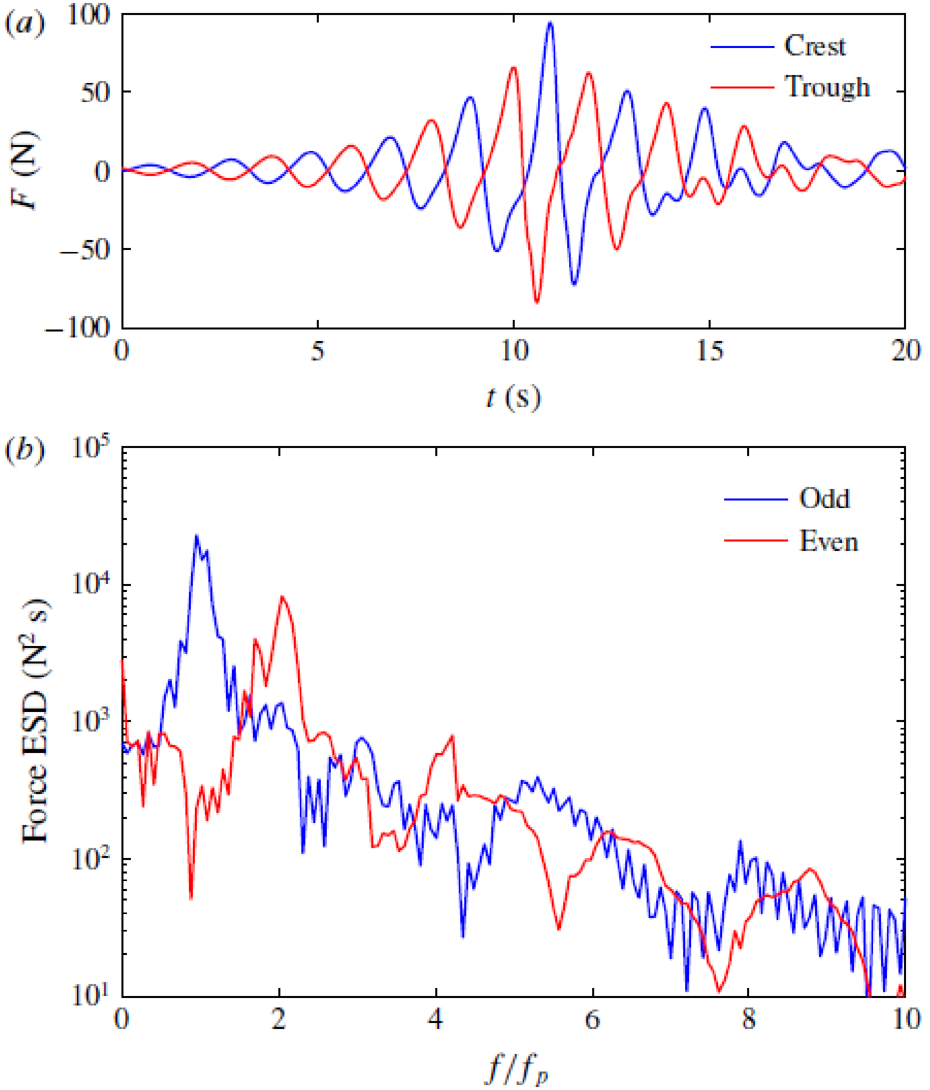
(a)
Crest
Trough
F (N)
t (s)
(b)
Odd
Even
Force ESD (N² s)
f / fp

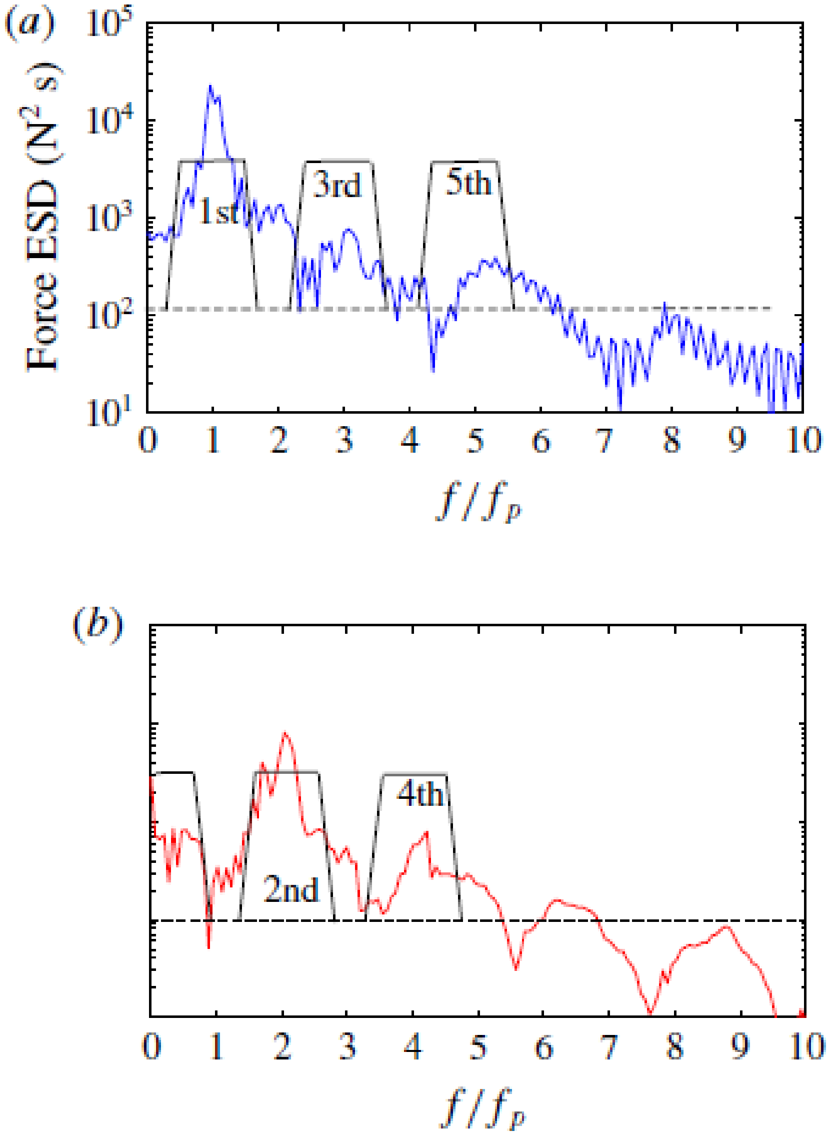
(a)
Force ESD (N² s)
1st
3rd
5th
f / fp
(b)
2nd
4th
f / fp

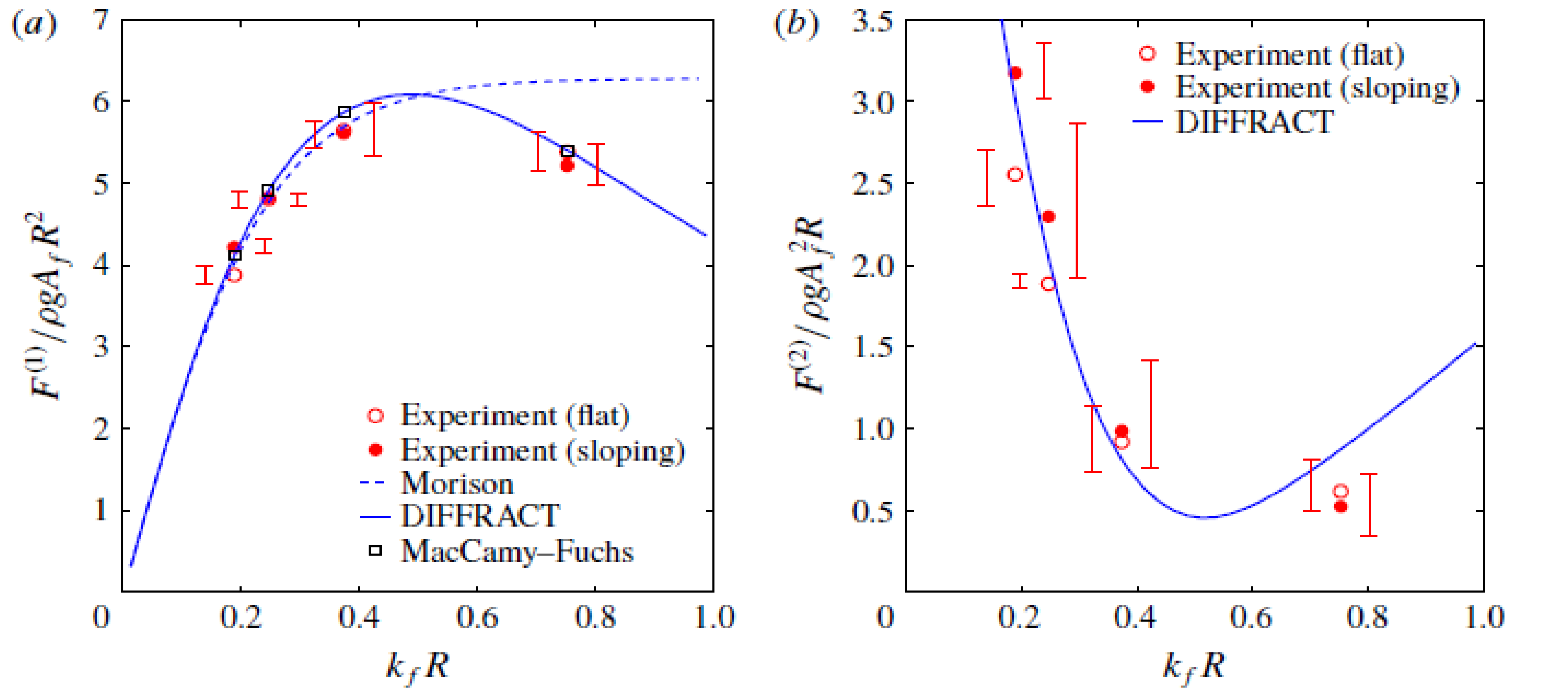

FIGURE 19. (Colour online) Variation of non-dimensional first- and second-order force harmonics with the cylinder size $k_f R$. (*a*) First-order force harmonic; (*b*) second-order force harmonic.

Linear force component

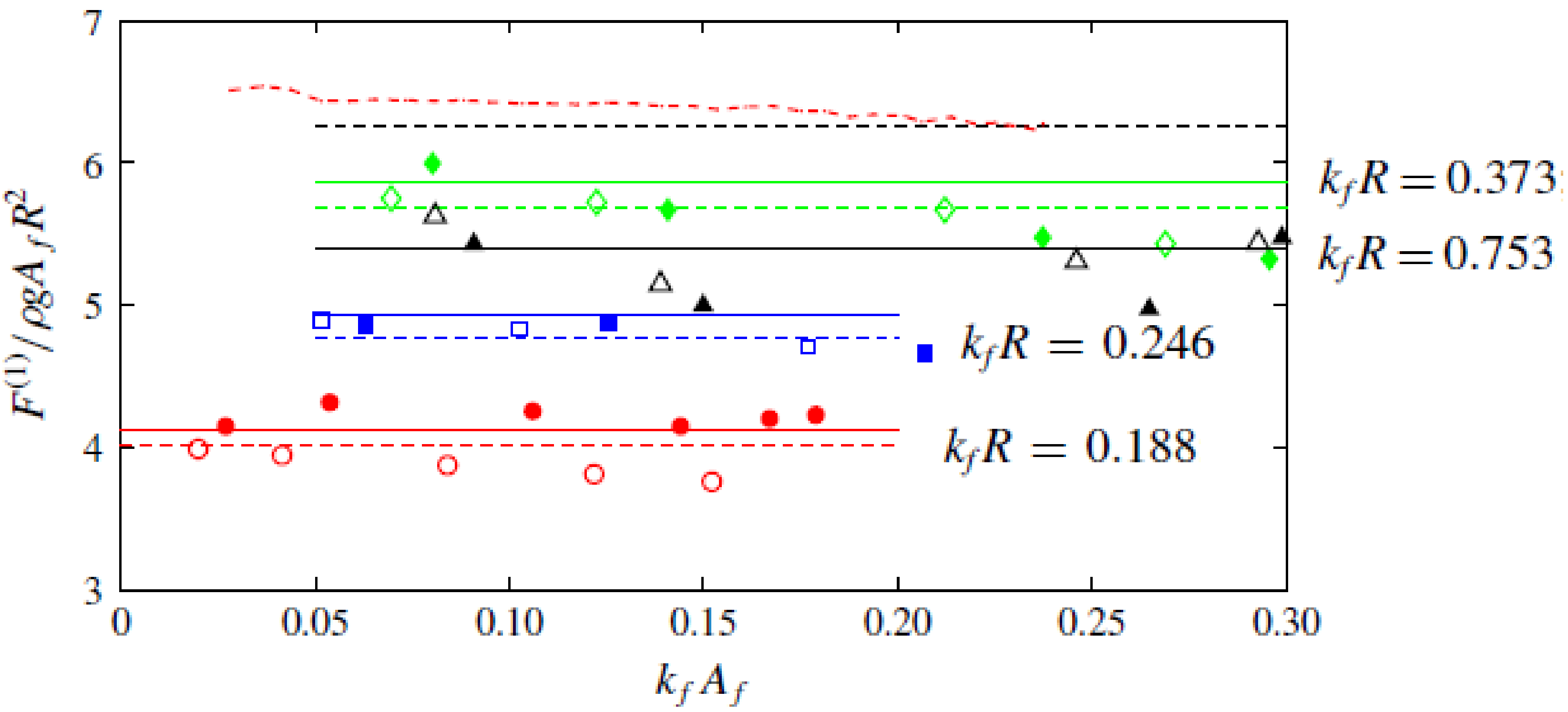

Solid line – DIFFRACT,

Dashed line – Morison Eq

Dot-dashed line – experiments from Huseby and Grue with $k_f R = 0.245$

Solid symbols – present experiments for sloping bed

Open symbols – present experiments for flat bed

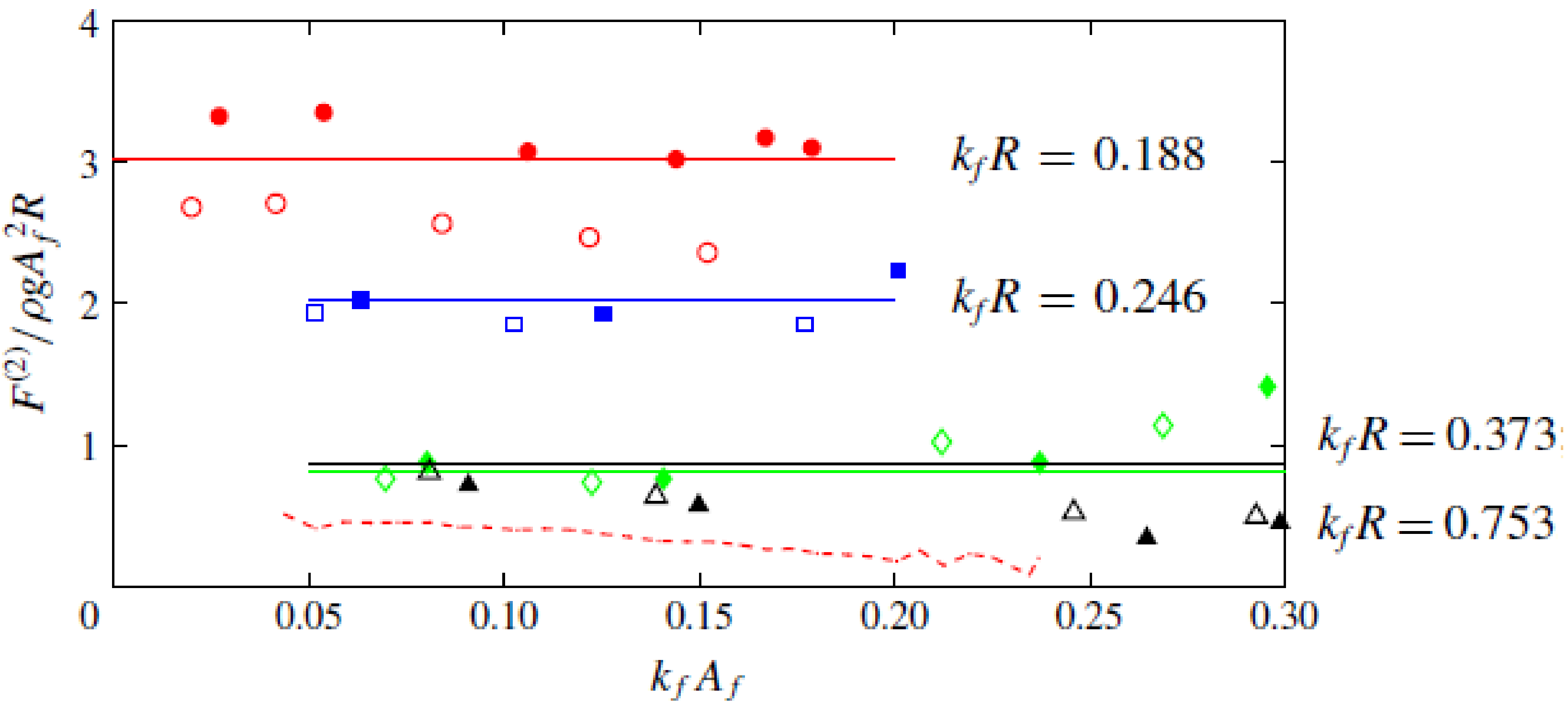

Solid line – DIFFRACT,

Dot-dashed line – experiments from Huseby and Grue with $k_f R = 0.245$.

Solid symbols – present experiments for sloping bed

Open symbols – present experiments for flat bed

Third-order harmonic forces

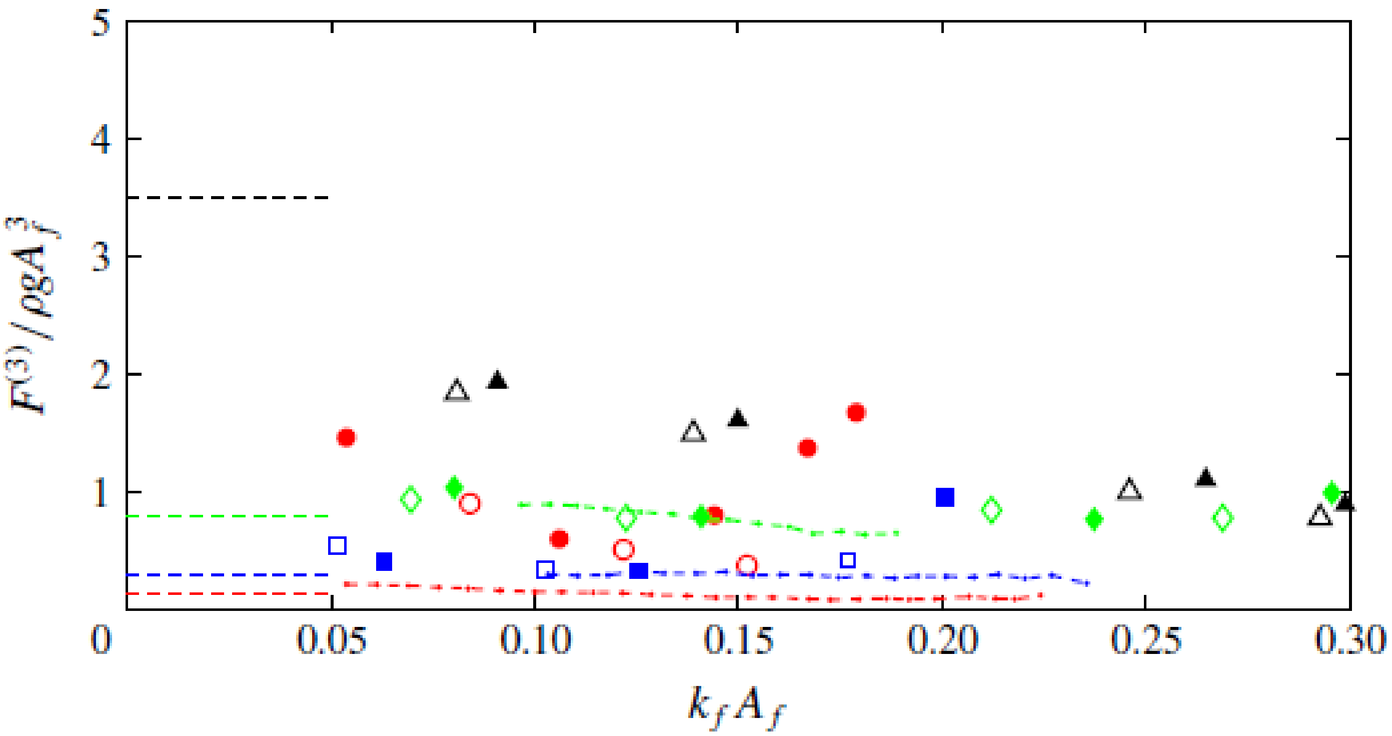

,

Dot-dashed line – experiments from Huseby and Grue with $k_f R = 0.245$.

Dash line - FNV solution

Solid symbols – present experiments for sloping bed

Open symbols – present experiments for flat bed

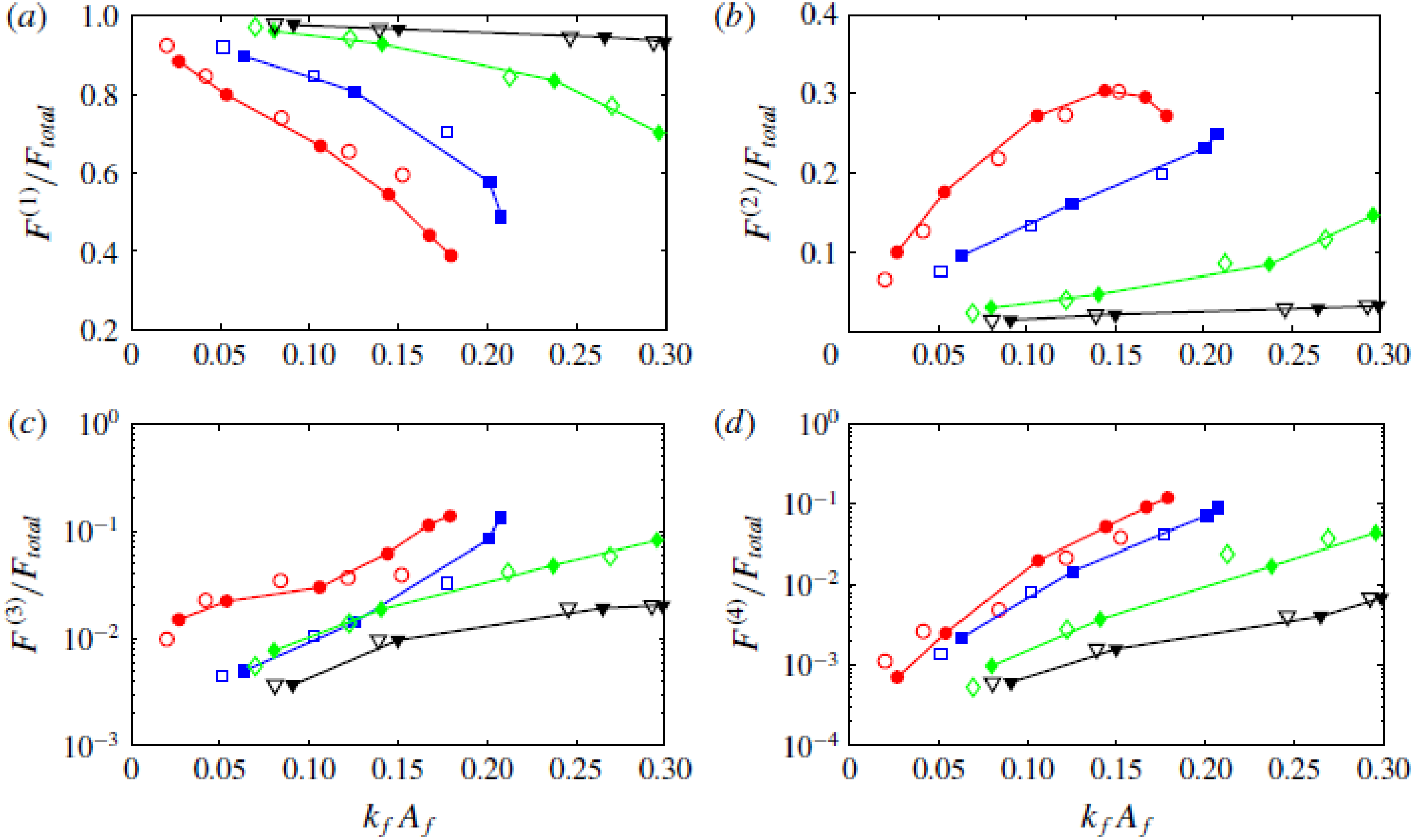

(a)
(b)
(c)
(d)
$F^{(1)}/F_{total}$
$F^{(2)}/F_{total}$
$F^{(3)}/F_{total}$
$F^{(4)}/F_{total}$
$k_f A_f$
$k_f A_f$

Flat bed

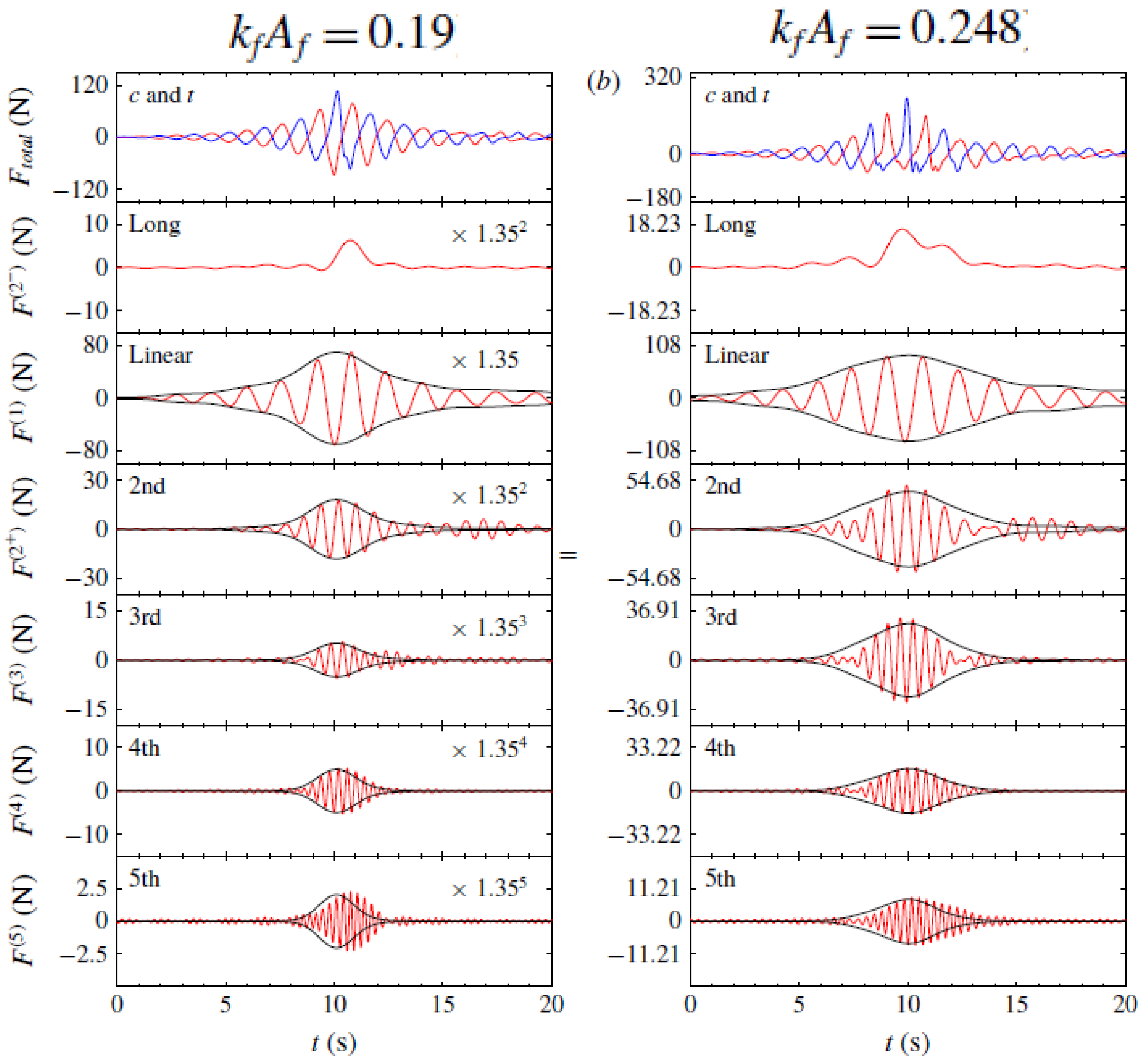

$f_p = 0.61$ Hz

1. The total in-line hydrodynamic force can be calculated by

$$\frac{F}{\rho g R^3} = S_{FE1}\left(\frac{A}{R}\right)[\alpha_{FE1}\eta_1 + \beta_{FE1}\eta_{1H}] + S_{FE2}\left(\frac{A}{R}\right)^2[\alpha_{FE2}(\eta_1^2 - \eta_{1H}^2) + \beta_{FE2}(2\eta_1\eta_{1H})] + \cdots$$

2. The alternative version where the phase functions are based on the linear force component

$$\frac{F}{\rho g R^3} = S_{FE1}\left(\frac{A}{R}\right)[\alpha_{FF1}f_1 + \beta_{FF1}f_{1H}] + S_{FE2}\left(\frac{A}{R}\right)^2[\alpha_{FF2}(f_1^2 - f_{1H}^2) + \beta_{FF2}(2f_1 f_{1H})] + \cdots .$$

Our hypothetical form for the entire harmonic structure can be written in terms of the linear component of force alone, with no reference to the associated undisturbed free-surface elevation at the position of the loaded cylinder. We write the linear component as

$$F_1 = \mathcal{F}_1 f_1$$

Where $\mathcal{F}_1$ is the peak value of the envelope of F_1 f_1 carries all the phase information. The total force in time becomes

$$\begin{aligned}\frac{F}{\rho g R^3} &= \frac{\mathcal{F}_1}{\rho g R^3}[f_1] + S_{FF2}\left(\frac{\mathcal{F}_1}{\rho g R^3}\right)^2[\alpha_{FF2}(f_1^2 - f_{1H}^2) + \beta_{FF2}(2f_1 f_{1H})] \\ &\quad + S_{FF3}\left(\frac{\mathcal{F}_1}{\rho g R^3}\right)^3[\alpha_{FF3}f_1(f_1^2 - 2f_{1H}^2) + \beta_{FF3}(f_{1H}(3f_1^2 - f_{1H}^2))] + \cdots .\end{aligned}$$

S_{FFn} is non-dimensional Coefs at each order, $(\alpha_{FFn}, \beta_{FFn})$- phase Coefs

New approach for predicting nonlinear wave loading

1. **Given free surface and linear wave forc**e,

Predict high order wave forces by

$$\frac{F}{\rho g R^3} = S_{FE1}\left(\frac{A}{R}\right)[\alpha_{FF1}f_1 + \beta_{FF1}f_{1H}] + S_{FE2}\left(\frac{A}{R}\right)^2[\alpha_{FF2}(f_1^2 - f_{1H}^2) + \beta_{FF2}(2f_1 f_{1H})] + \cdots .$$

Flat bed

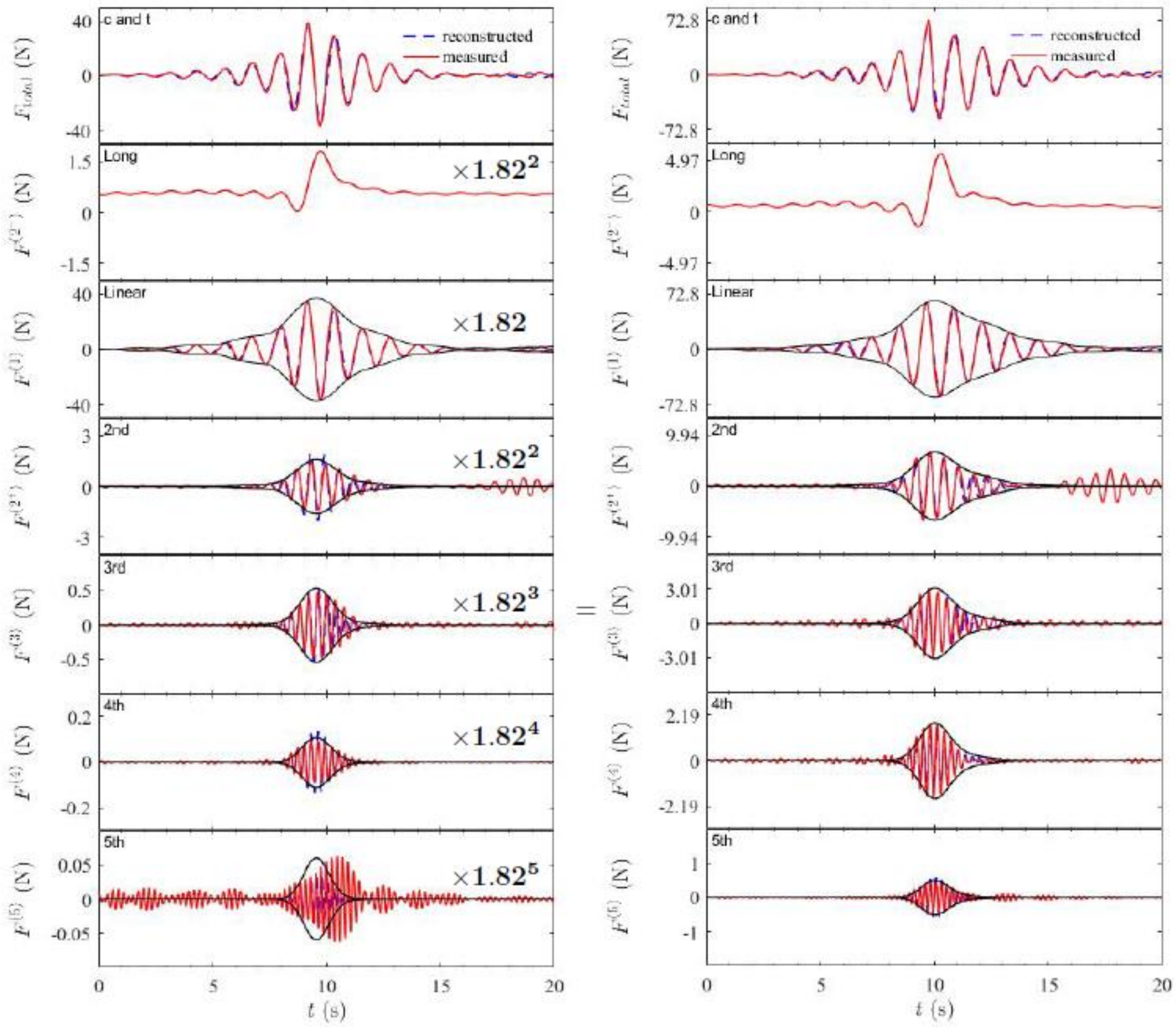

c and t
reconstructed
measured
Long
Linear
2nd
3rd
4th
5th
×1.82²
×1.82
×1.82³
×1.82⁴
×1.82⁵
=
t (s)

Sloping bed

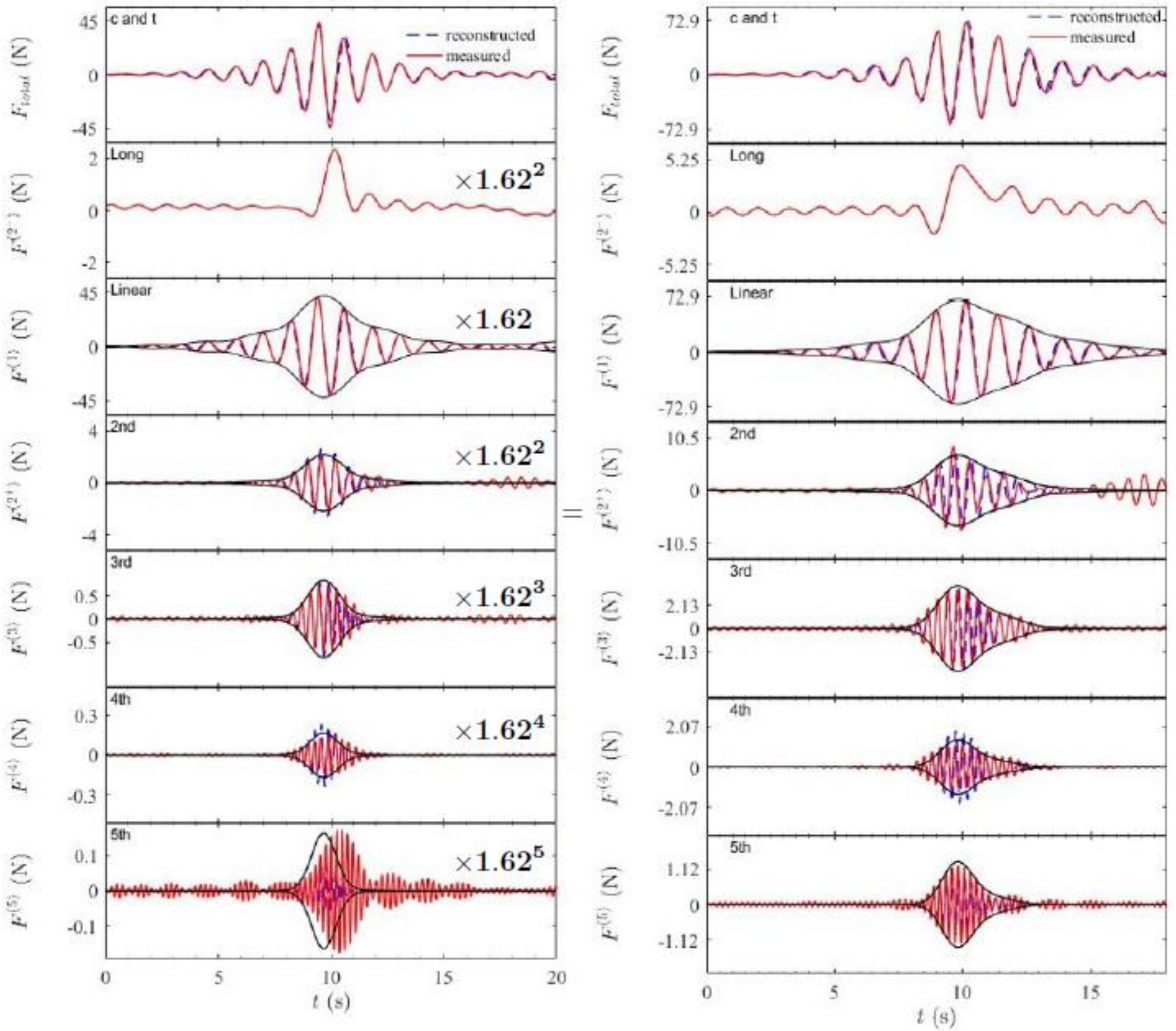

c and t
reconstructed
measured
F_{total} (N)
Long
$\times 1.62^2$
$F^{(2^-)}$ (N)
Linear
$\times 1.62$
$F^{(1)}$ (N)
2nd
$\times 1.62^2$
$F^{(2^+)}$ (N)
3rd
$\times 1.62^3$
$F^{(3)}$ (N)
4th
$\times 1.62^4$
$F^{(4)}$ (N)
5th
$\times 1.62^5$
$F^{(5)}$ (N)
t (s)
=

New approach for predicting nonlinear wave loading

2. Given linear wave force only,

predict high order wave forces

$$F_1 = \mathcal{F}_1 f_1$$

$$\frac{F}{\rho g R^3} = \frac{\mathcal{F}_1}{\rho g R^3}[f_1] + S_{FF2}\left(\frac{\mathcal{F}_1}{\rho g R^3}\right)^2 [\alpha_{FF2}(f_1^2 - f_{1H}^2) + \beta_{FF2}(2 f_1 f_{1H})]$$
$$+ S_{FF3}\left(\frac{\mathcal{F}_1}{\rho g R^3}\right)^3 [\alpha_{FF3} f_1 (f_1^2 - 2 f_{1H}^2) + \beta_{FF3}(f_{1H}(3 f_1^2 - f_{1H}^2))] + \cdots .$$

S_{FFn} is non-dimensional Coefs at each order, $(\alpha_{FFn}, \beta_{FFn})$ - phase Coefs

Sloping bed

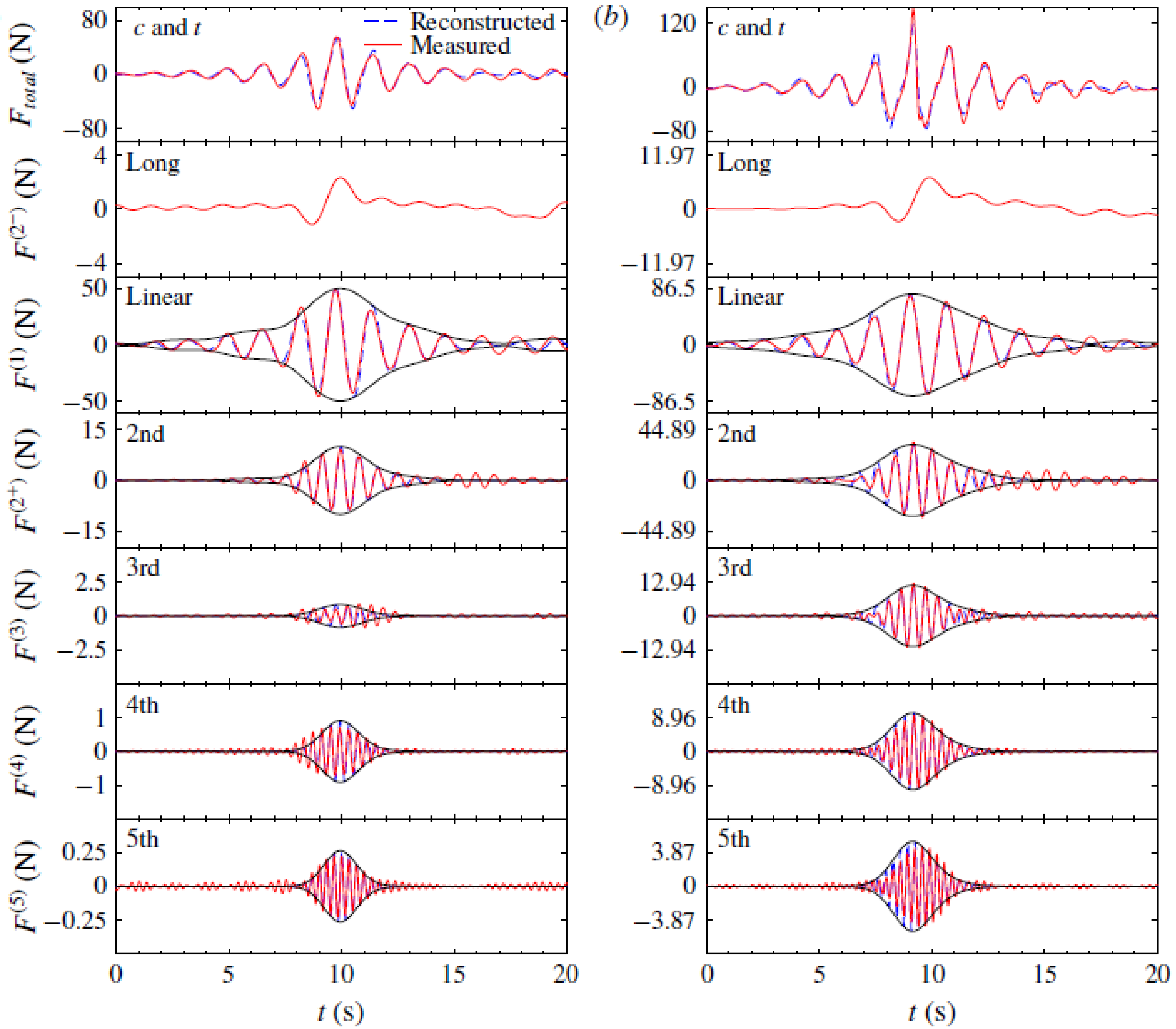

(b)
c and t
Reconstructed
Measured
Long
Linear
2nd
3rd
4th
5th
F_{total} (N)
$F^{(2-)}$ (N)
$F^{(1)}$ (N)
$F^{(2+)}$ (N)
$F^{(3)}$ (N)
$F^{(4)}$ (N)
$F^{(5)}$ (N)
t (s)

Observations and summary

UNIVERSITY OF BATH

Our experiments on wave impact on mono-pile have found that

- The strongly non-linear harmonic force components can be separated by applying the ‘phase-inversion’ method to the measured force time histories. It works well even for locally violent nearly-breaking waves formed from bidirectional wave pairs.
- The nth-harmonic force scales with the nth power of the envelope of both the linear undisturbed free-surface elevation and the linear force component in both time variation and amplitude.
- **This allows estimation of the higher-order harmonic shapes and time histories from knowledge of the linear component alone!**
- The experiments also show that the harmonic structure of the wave loading on the cylinder is virtually unaltered by the introduction of a sloping bed, depending only on the local wave properties at the cylinder.
- **Nonlinear forces on a column high-order harmonics contribute more than 60% of the loading**. The significance of this striking new result is that it reveals the importance of high-order nonlinear wave loading on offshore structures and means that such loading should be considered in their design.

Access to the experimental data

Some of the selected experimental data for our experiments on focused wave interaction with a circular cylinder have been made open access.

Below is the link to download the data, which is included in the CCP-WSI webpage.

https://www.ccp-wsi.ac.uk/data_repository/test_cases/test_case_008

Wave interaction with vertical cylinder

Test Case ID: 8
Date of Experiment: 1 Sep 2009
Dynamics of Fluids: Regular Waves, Focused/Design Waves
Structures, Devices & Obstacles: Coastal Structures, Offshore Structures
Project: Breaking wave impacts and non-breaking wave interactions with offshore wind turbine foundations
Institution: University of Bath
Facility: Danish Hydraulic Institute (DHI)
Contact: Dr Jun Zang (J.Zang@bath.ac.uk)

UNIVERSITY OF BATH

Relevant References

Move to top

Chen, LF, Zang, J, Hillis, AJ, Morgan, GCJ & Plummer, AR 2014, 'Numerical investigation of wave-structure interaction using OpenFOAM', Ocean Engineering, vol. 88, pp. 91-109. https://doi.org/10.1016/j.oceaneng.2014.06.003

Chen, L, Zang, J, Taylor, PH, Sun, L, Morgan, G, Grice, J, Orszaghova, J & Tello, M 2018a, 'An experimental decomposition of nonlinear forces on a surface-piercing column: Stokes-type expansions of the force harmonics', Journal of Fluid Mechanics, vol. 848, pp. 42-77. https://doi.org/10.1017/jfm.2018.339

Chen, Q, Zang, J, Kelly, DM & Dimakopoulos, A 2018b, 'A 3D parallel Particle-In-Cell solver for wave interaction with vertical cylinders', Ocean Engineering, vol. 147, pp. 165-180. https://doi.org/10.1016/j.oceaneng.2017.10.023

Zang, J., Taylor, P.H., Morgan, G.C.J., Stringer, R., Orszaghova, J., Grice, J. and Tello, M. 2010. Steep wave and breaking wave impact on offshore wind turbine foundations – ringing revisited. The 25th International Workshop on Water Waves and Floating Bodies. http://www.iwwwfb.org/Abstracts/iwwwfb25/iwwwfb25_52.pdf

Zang, J., Taylor, P.H., Morgan, G.C.J., Tello, M., Grice, J. and Orszaghova, J. 2010. Experimental study of non-linear wave impact on offshore wind turbine foundations. Coastlab10 – the 3rd International Conference on the Application of Physical Modelling to Port and Coastal Protection.

Comparisons of numerical modelling of some of the experiments

1. **2^{nd} – order Potential flow theory** (In-house code)

2. **N-S solver – OpenFOAM** (open source)

3. **Hybrid N-S solver – Particle–In-Cell method** (In-house code)

Why do we choose these three numerical methods?

1. Second-order Potential Flow Model:

DIFFRACT

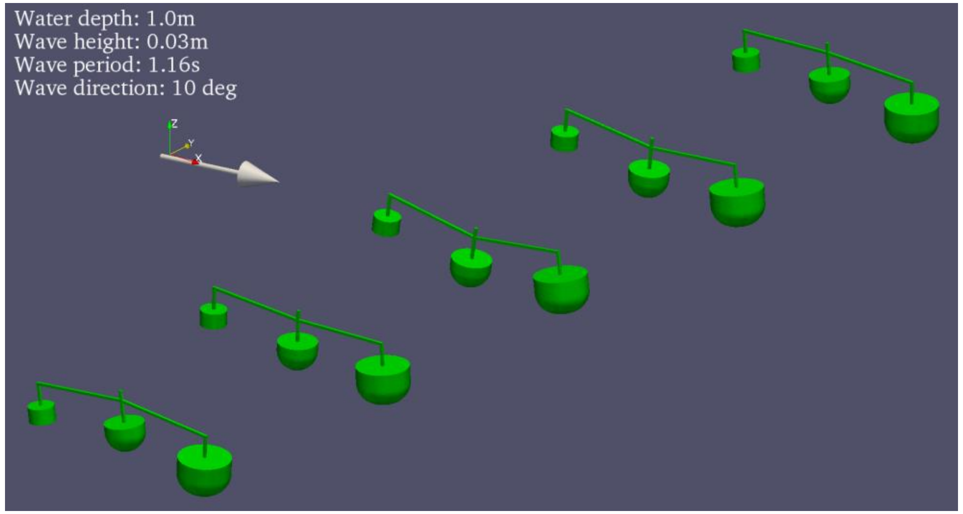

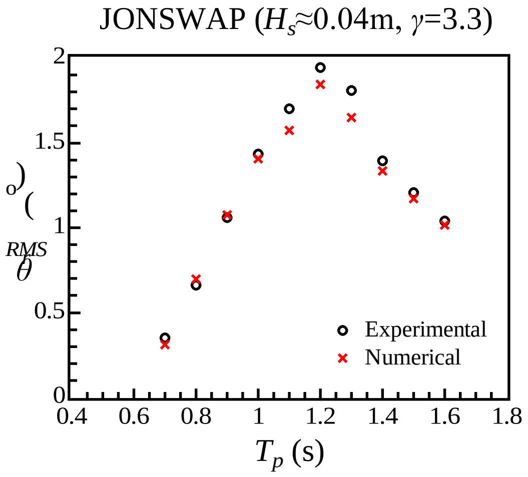

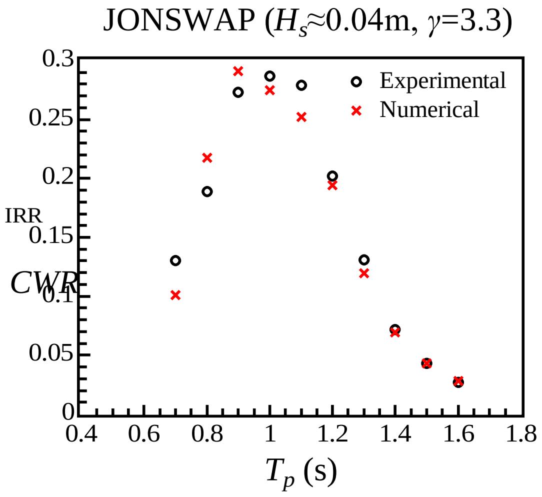

2. CFD open source model: OpenFOAM

Regular wave propagation over a submerged bar, The test case is based on experiments by Beji and Battjes (1993) and Luth (1994)

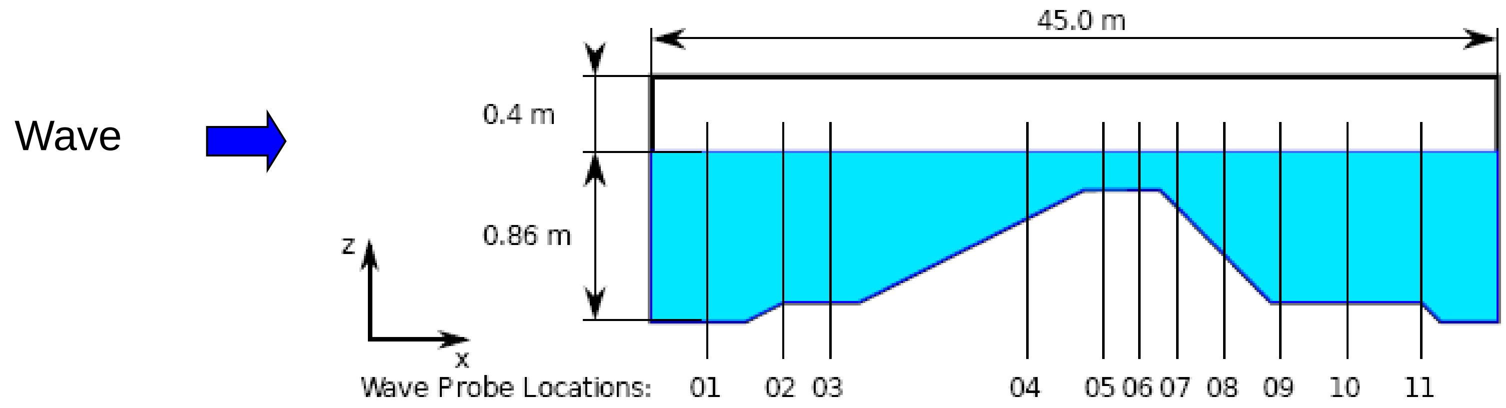

Morgan, G.C.J., Zang, J., Greaves, D., Heath, A., Whitlow, C. and Young, J., 2010

Using the rasInterFoam CFD model for wave transformation and coastal modelling. *Proceeding of Coastal Engineering.* American Society of Civil Engineers, pp. 418-423.

Free surface

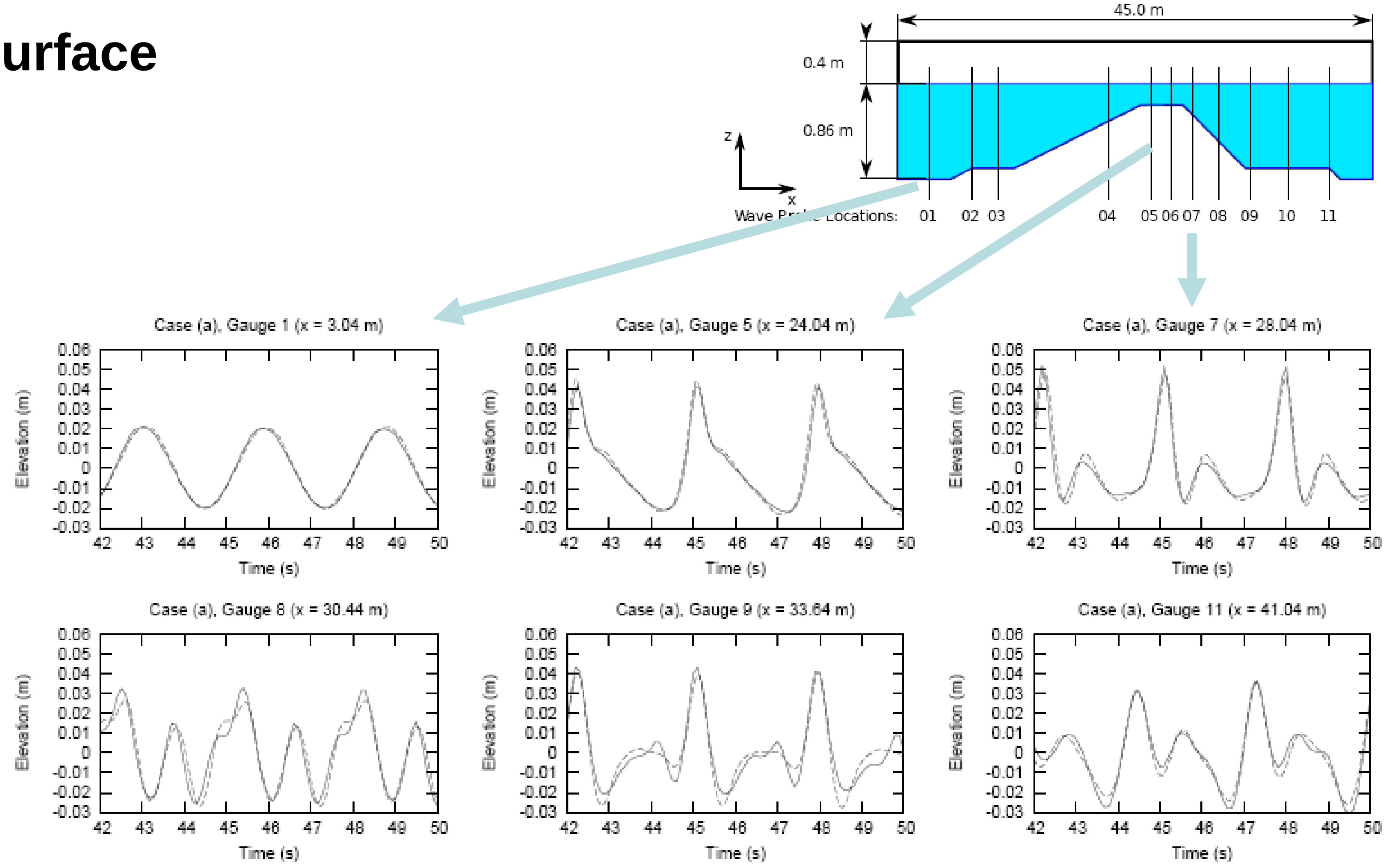

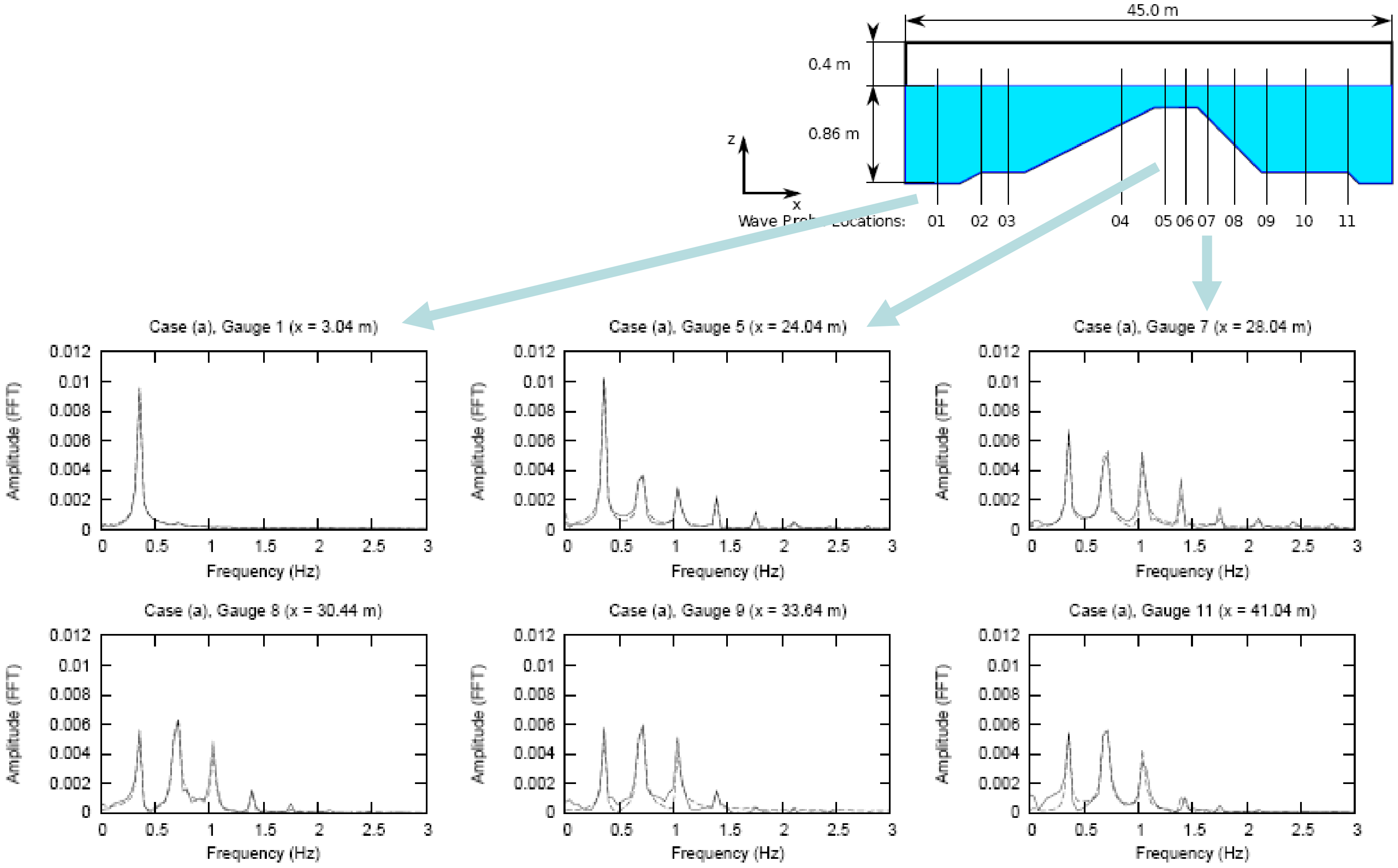
45.0 m
0.4 m
0.86 m
z
x
Locations:
01 02 03 04 05 06 07 08 09 10 11
Case (a), Gauge 1 (x = 3.04 m)
Case (a), Gauge 5 (x = 24.04 m)
Case (a), Gauge 7 (x = 28.04 m)
Case (a), Gauge 8 (x = 30.44 m)
Case (a), Gauge 9 (x = 33.64 m)
Case (a), Gauge 11 (x = 41.04 m)
Amplitude (FFT)
Frequency (Hz)
0 0.002 0.004 0.006 0.008 0.01 0.012
0 0.5 1 1.5 2 2.5 3

3. PIC Method

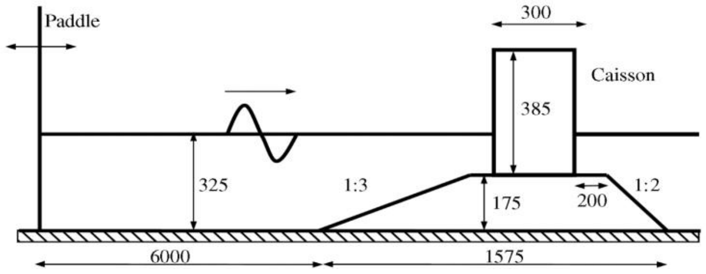

Moving breakwater

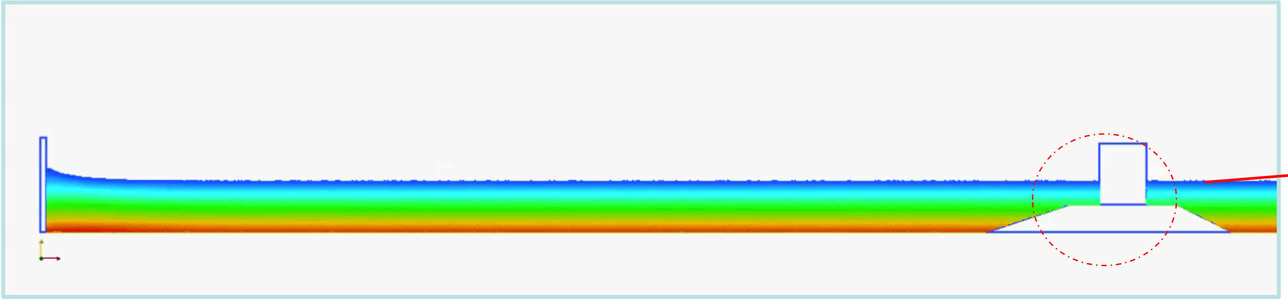

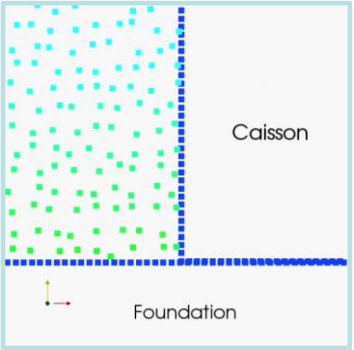

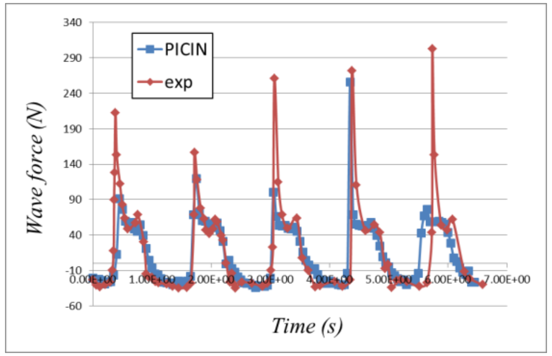

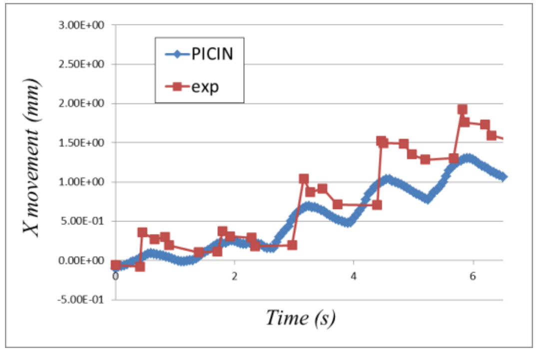

37,000 cells and 64,000 particles, ~1.44 hrs for 15s of simulation on an Intel(R) i5-3470 CPU @ 3.2GHz core.

Regular wave

$kR = 2\pi a/L$ (slenderness) = 0.37 ; $kA = 2\pi A/L$ (steepness) = 0.2

Wave Run-up

Wave force

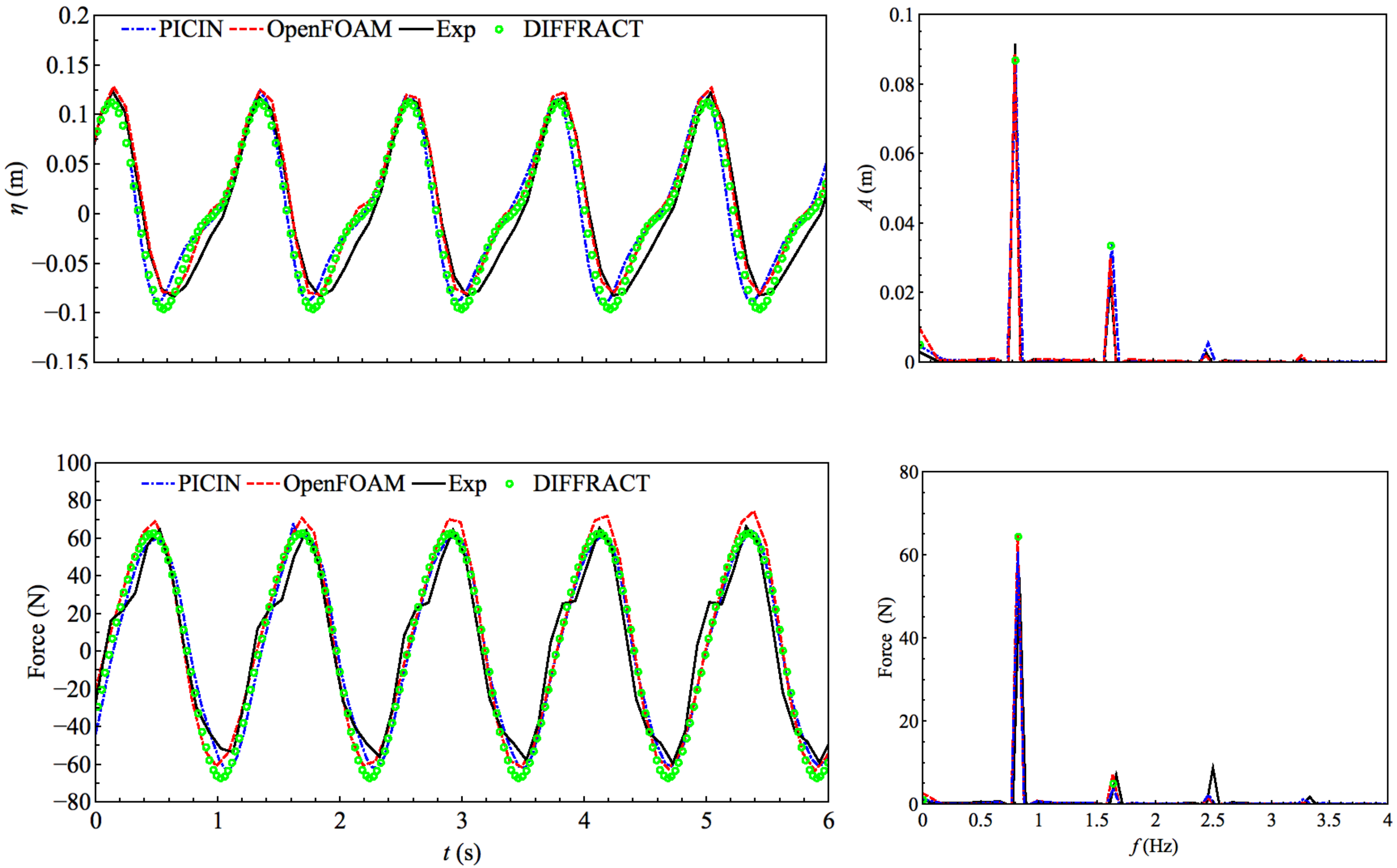

Regular wave

$ka = 2\pi a/L$ (slenderness) = 0.37 ; $kA = 2\pi A/L$ (steepness) = 0.2

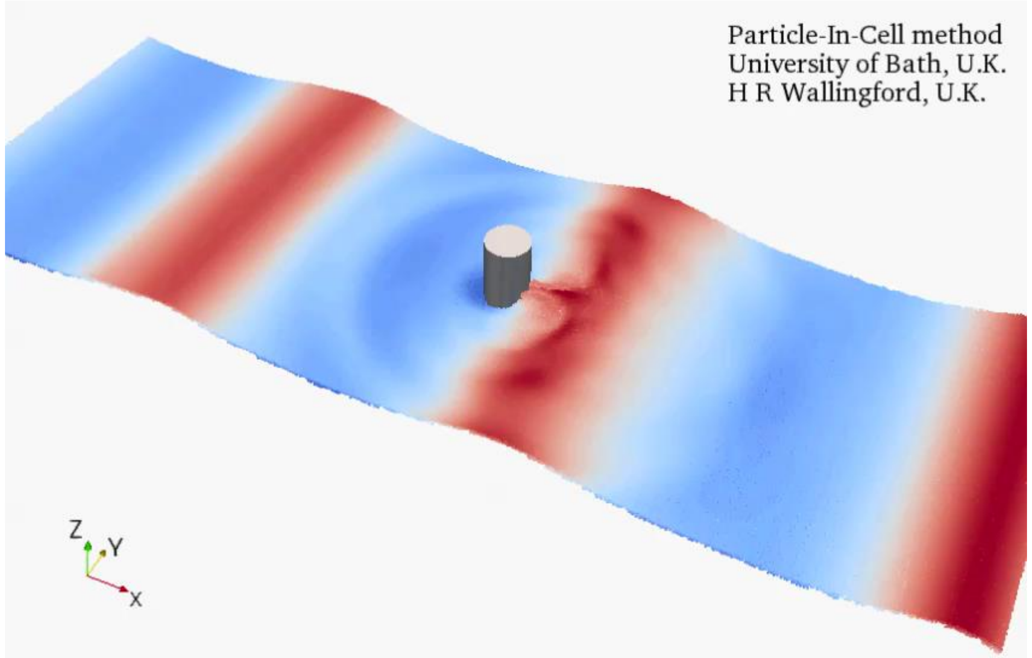

Focussed wave

$kR = 2\pi a/L$ (slenderness) = 0.25 ; $kA = 2\pi A/L$ (steepness) = 0.2

Wave Run-up

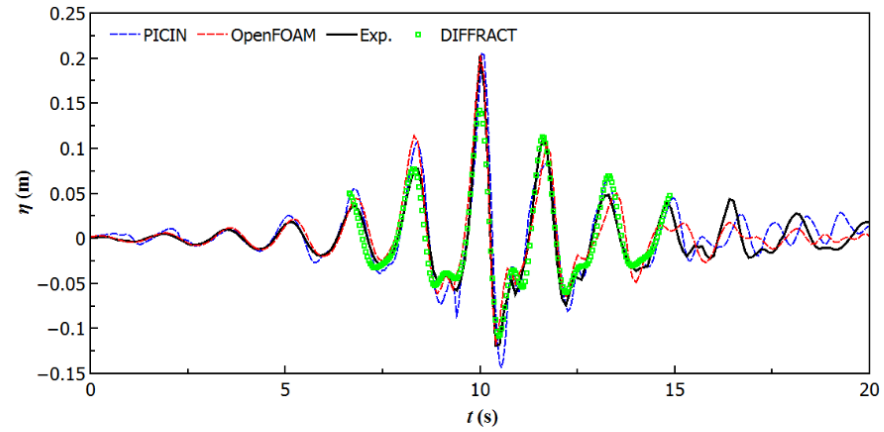

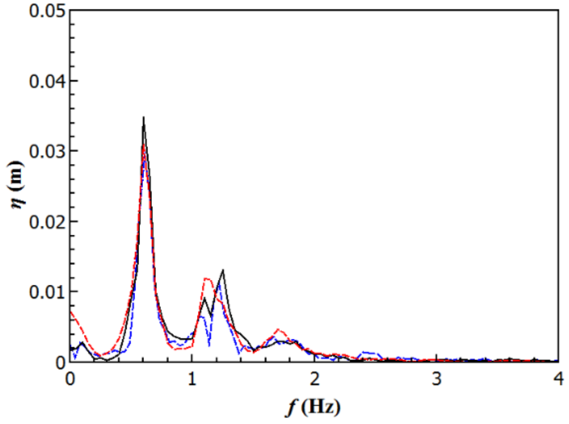

Wave force

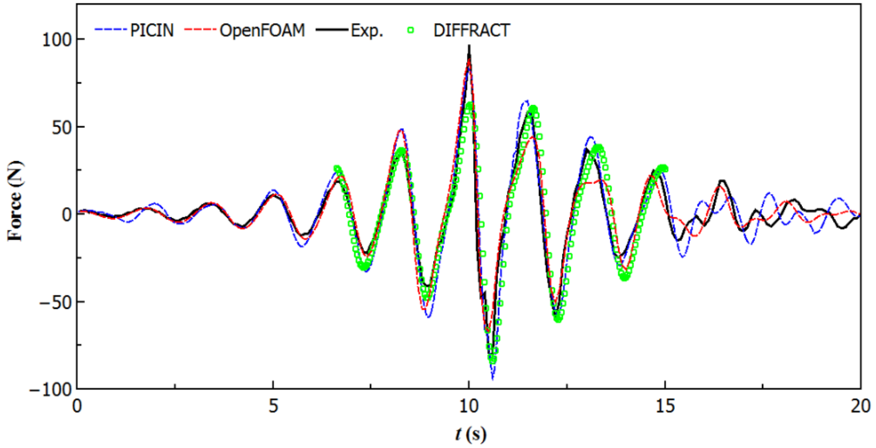

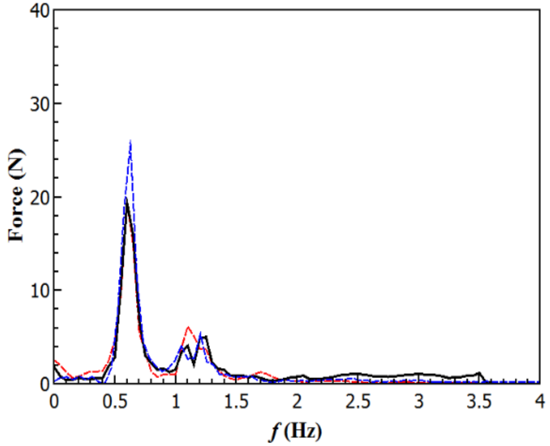

Focused wave

$ka = 2\pi a/L$ (slenderness) = 0.25 ; $kA = 2\pi A/L$ (steepness) = 0.2

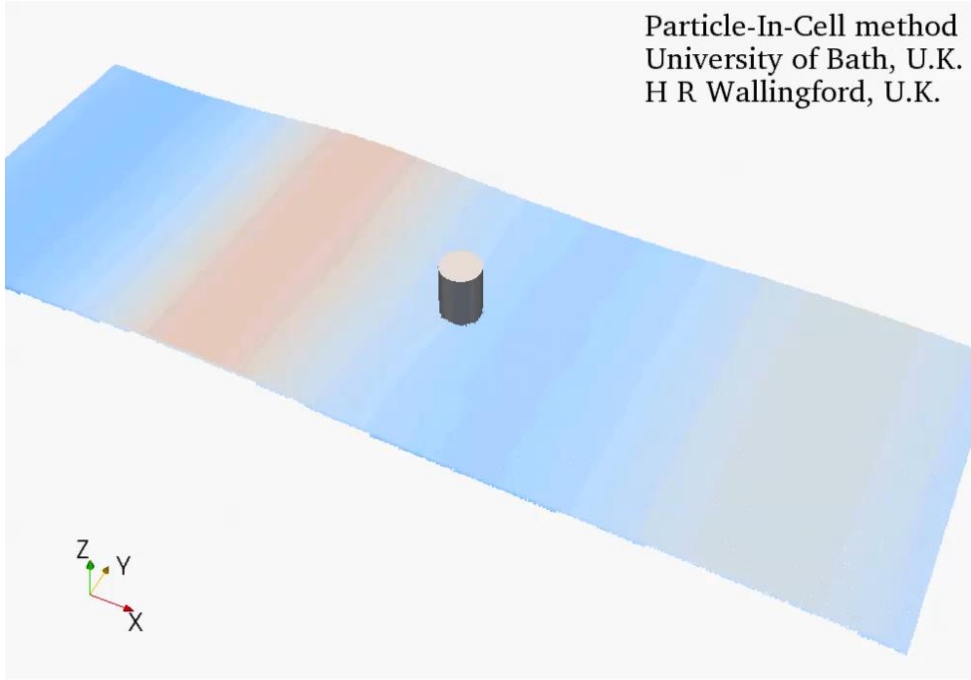

Scattered wave field

Numerical simulation

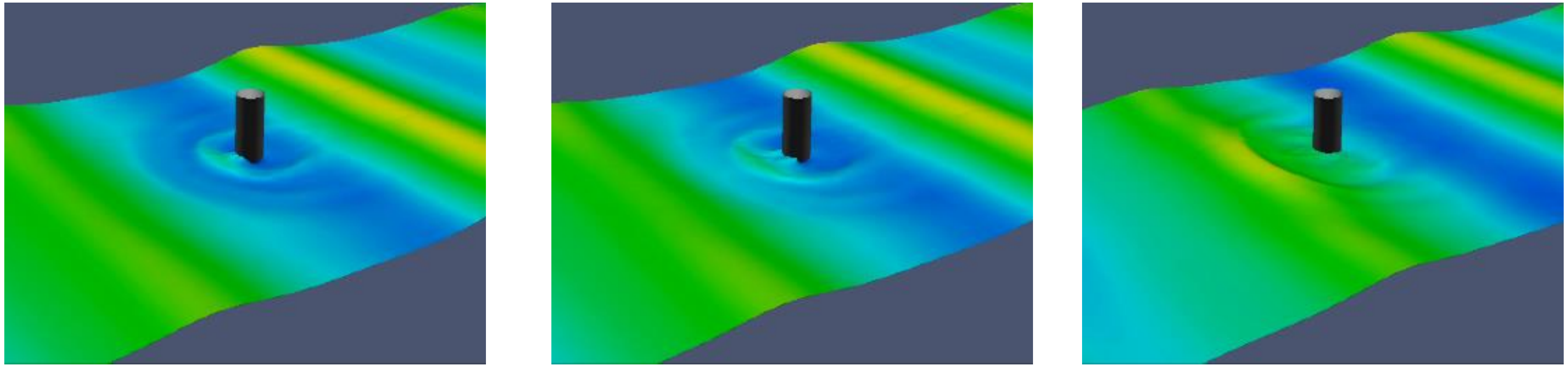

Experiment at Imperial College

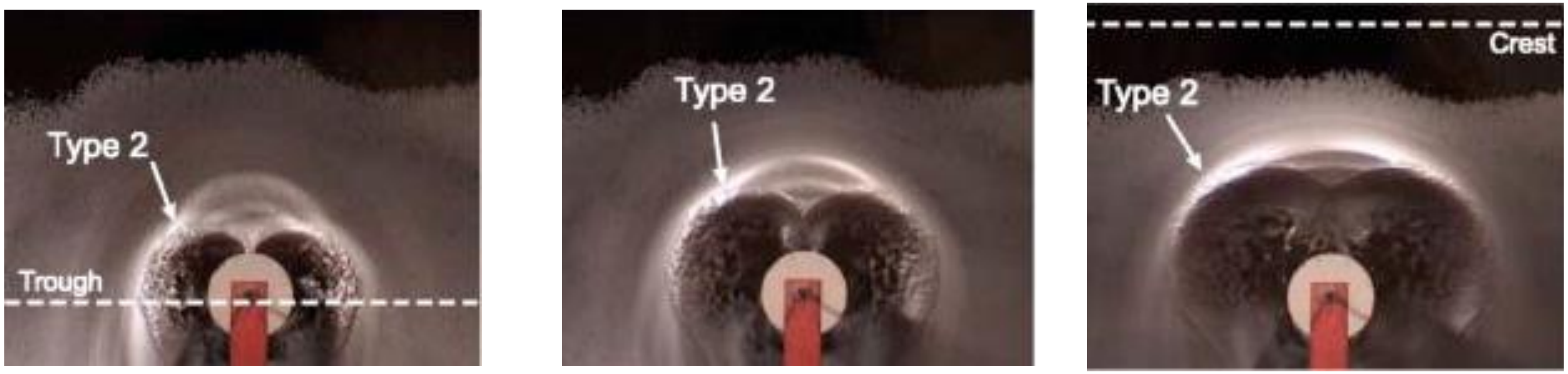

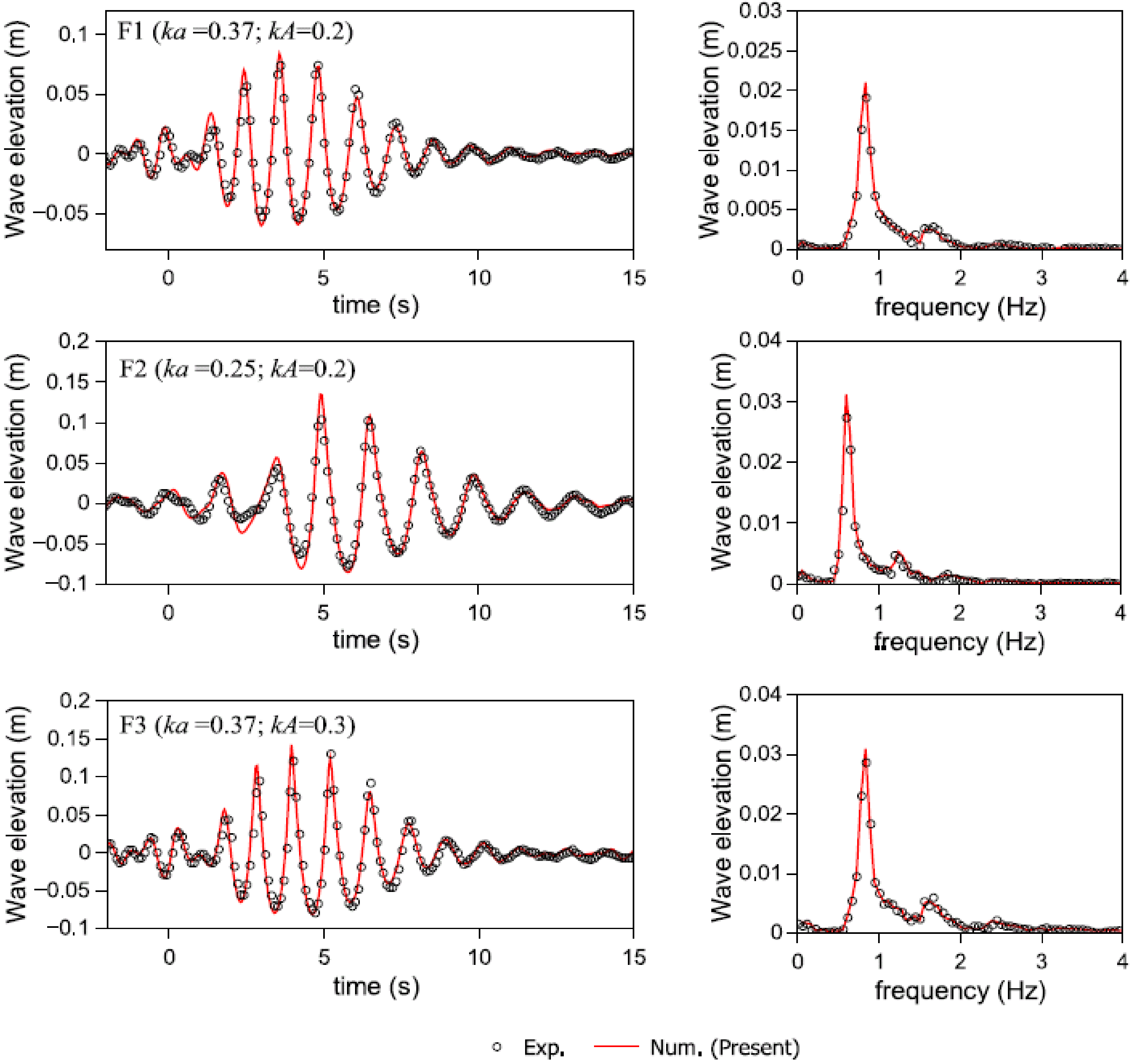

F1 (ka =0.37; kA=0.2)
F2 (ka =0.25; kA=0.2)
F3 (ka =0.37; kA=0.3)
Wave elevation (m)
time (s)
frequency (Hz)
Exp.
Num. (Present)

Items	"full particle" PIC	OpenFOAM
Cell number n (million)	9.20	8.33
Cores p	80	8
Simulated time t_s (T)	18.0	24.5
Total CPU time C_t (h)	12.16	126.20
Magnified CPU cost: $\frac{p \times C_t}{n \times t_s}$	5.87	4.95

Potential flow theory: Very fast!

Observations and summary

Recent developments of advanced numerical methods have revealed that

- Different numerical methods have shown their own merits and disadvantages.

- Potential flow model (like DIFFRACT, WAMIT) is efficient, but may have limitations in simulating highly nonlinear effects. Make good use of the potential flow solvers, but we have to understand their limits.

- Novel efficient viscous numerical methods (like PICIN, OpenFOAM and SPH etc) provided great potential for simulating complex free surface flows and their interactions with coastal and offshore structures.

- Depending on what we need and at what cost: choosing a numerical method should be closely related to the nature of the problem, the requirement for the solutions and the resources we have.

Thank you!

Dr. Jun Zang J.Zang@bath.ac.uk

Thanks to: L Chen, L Sun, Q Chen, DZ Ning, SX Liu, J Li, G Morgan, J Grice, J Orszaghova, M Tello Ruiz, B Teng, PH Taylor, R Eatock Taylor, …….

The "face" of Neptune appears over Newhaven harbour wall, 6 July 2021

The sighting of the "face" of the Roman god of water was captured by BBC photographer Jeff Overs in Newhaven on Tuesday, 6 July 2021.
(Reported by BBC)